BIOMEDICAL ENGINEERING

10.1126/sciadv.1500439

Nanodiamonds: The intersection of nanotechnology, drug development, and personalized medicine

Dean Ho,[1,2,3,4,5]* Chung-Huei Katherine Wang,[6] Edward Kai-Hua Chow[7,8,9]*

The implementation of nanomedicine in cellular, preclinical, and clinical studies has led to exciting advances ranging from fundamental to translational, particularly in the field of cancer. Many of the current barriers in cancer treatment are being successfully addressed using nanotechnology-modified compounds. These barriers include drug resistance leading to suboptimal intratumoral retention, poor circulation times resulting in decreased efficacy, and off-target toxicity, among others. The first clinical nanomedicine advances to overcome these issues were based on monotherapy, where small-molecule and nucleic acid delivery demonstrated substantial improvements over unmodified drug administration. Recent preclinical studies have shown that combination nanotherapies, composed of either multiple classes of nanomaterials or a single nanoplatform functionalized with several therapeutic agents, can image and treat tumors with improved efficacy over single-compound delivery. Among the many promising nanomaterials that are being developed, nanodiamonds have received increasing attention because of the unique chemical-mechanical properties on their faceted surfaces. More recently, nanodiamond-based drug delivery has been included in the rational and systematic design of optimal therapeutic combinations using an implicitly de-risked drug development platform technology, termed Phenotypic Personalized Medicine–Drug Development (PPM-DD). The application of PPM-DD to rapidly identify globally optimized drug combinations successfully addressed a pervasive challenge confronting all aspects of drug development, both nano and non-nano. This review will examine various nanomaterials and the use of PPM-DD to optimize the efficacy and safety of current and future cancer treatment. How this platform can accelerate combinatorial nanomedicine and the broader pharmaceutical industry toward unprecedented clinical impact will also be discussed.

INTRODUCTION

Over the past several decades, substantial progress toward improving cancer treatment outcomes has been made because of advances in drug compounds that can improve tumor-targeting efficacy and safety. A broad spectrum of nanomaterials has been used for pioneering cancer treatment studies that have been validated from in vitro to in vivo to clinical trials. These include poly(lactic-co-glycolic acid) (PLGA), metallic nanoparticles, carbon nanotubes (CNTs), polymer-based materials, and lipid-based materials, among many others (*1*–*12*). Clinical trials using PLGA-docetaxel nanoparticles have demonstrated efficacy in tonsillar cancer therapy, first-in-human trials using small interfering RNA (siRNA)–cyclodextrin compounds resulted in clinically validated RNA interference, and a clinical trial for gold nanoshell–based photothermal ablation therapy against head and neck cancer has recently been completed (*3*, *13*).

Among the nanomaterials that are being developed for clinical therapeutic applications, carbon-based nanomaterials are being increasingly studied as drug delivery and bioimaging agents. Carbon-based nanomaterials evaluated for biomedical applications include CNTs, graphene, fullerenes, carbon nanospheres, and carbon dots, among others. Studies have shown that these carbon-based nanomaterials can be easily functionalized to deliver a wide range of therapeutics and are well tolerated in acute toxicity studies (*14*–*18*). Additionally, a number of these carbon-based nanomaterials have intrinsic properties that can be harnessed in imaging applications (*19*–*21*). Detonation nanodiamonds (DND) and fluorescent nanodiamonds (FNDs), in particular, have piqued interest in the biomedical community because of their several favorable properties (*22*–*35*). For example, NDs have unique faceted surfaces, and their importance in biological and medical applications was initially elucidated on the basis of the seminal work by Barnard and colleagues (*22*, *36*–*39*). Additionally, facet-specific electrostatics have played a role in coordinating water molecules around the ND surface. This led to remarkably high relaxivity values being observed after the conjugation of gadolinium(III) to ND particles (*40*). At values approaching 60 mM^{-1} s^{-1}, which are one order of magnitude greater than clinical standards, ND-gadolinium(III) complexes produced the highest ever reported per-gadolinium values. These relaxivity measurements, attributed to water coordination around the ND facets, imply that a marked decrease in gadolinium dosing can be used in the clinic. In addition to this particularly unique approach to magnetic resonance imaging using NDs, other biomedical applications of NDs that have been previously explored include orthopedic engineering (*41*), the synthesis of contact lenses (*42*), single-cell magnetometry (*43*), toxicity studies in worms and rodents (*44*), cancer stem cell targeting (*45*), and targeted preclinical breast cancer therapy (*46*).

Given the significant costs associated with new drug development, it is becoming increasingly important to engineer nanomedicine therapies where the therapeutic and nanomaterial carriers are optimally suited for the intended indication. More specifically, stable drug loading,

[1]Division of Oral Biology and Medicine, University of California, Los Angeles (UCLA) School of Dentistry, Los Angeles, CA 90095, USA. [2]Department of Bioengineering, UCLA School of Engineering and Applied Science, Los Angeles, CA 90095, USA. [3]The Jane and Jerry Weintraub Center for Reconstructive Biotechnology, UCLA School of Dentistry, Los Angeles, CA 90095, USA. [4]California NanoSystems Institute, UCLA, Los Angeles, CA 90095, USA. [5]Jonsson Comprehensive Cancer Center, UCLA, Los Angeles, CA 90095, USA. [6]BRIM Biotechnology Inc., Taipei 11560, Taiwan, R.O.C. [7]Cancer Science Institute of Singapore, Yong Loo Lin School of Medicine, National University of Singapore, Singapore 117599, Singapore. [8]Department of Pharmacology, Yong Loo Lin School of Medicine, National University of Singapore, Singapore 177599, Singapore. [9]National University Cancer Institute, Singapore, Singapore 119082, Singapore.
*Corresponding author. E-mail: dean.ho@ucla.edu (D. H.); csikce@nus.edu.sg (E. K.-H. C.)

sustained drug elution, reduced off-target toxicity, enhanced efficacy over the clinical standard and other nanoparticle-drug formulations, scalable drug-nanomaterial integration, and confirmation of material safety are among the many criteria for continued development toward clinical implementation. More recently, multifunctional drug delivery using single nanoparticle platforms has been demonstrated. Examples include aptamer-based targeting coupled with small-molecule delivery as well as co-delivery of siRNA and small molecules to simultaneously down-regulate drug transporters that mediate resistance and mediate cell death (*1*, *47*, *48*). Layer-by-layer deposition of multiple drugs onto a single nanoparticle for breast cancer therapy has also been demonstrated (*49*). Adenosine triphosphate (ATP)–triggered therapeutic release and other hybrid delivery approaches have also been shown to be more effective in improving cancer therapy over conventional approaches (*50*, *51*). These and other breakthroughs in nanomedicine have made the need for combination therapy, or the ability to concurrently address multiple tumor proliferation mechanisms, clearly evident (*52*). Combination therapy represents a powerful standard of care, and if nanomedicine can markedly improve monotherapy over the administration of drugs alone, it is apparent that combination nanotherapy can further improve on what is currently being used in the clinic.

As the utility of nanomedicine in the clinical setting is becoming more apparent, new challenges pertaining to globally optimizing treatment have arisen. Conventional approaches to formulating unmodified drug combinations are based on additive design. This concept uses the initial combination of maximum tolerated doses (MTDs) for each drug and then adjusting each dose using a scaling factor to minimize toxicity while mediating an expected high level of efficacy. Given the nearly infinite number of combinations that are possible when a three-drug combination is being designed, additive design precludes combination therapy optimization. This is a long-standing challenge that has confronted the pharmaceutical industry and will undoubtedly need to be addressed by the nanomedicine community as well. As powerful genomics-based precision medicine approaches are being developed to potentially enable the design of tailored therapies, nanotechnology-modified drug development may be able to take advantage of patient genetics to improve treatment outcomes. In addition to genomics-based precision medicine, a recent example of mechanism-independent phenotypic optimization of combination therapy has been demonstrated. This approach systematically created ND-modified and unmodified drug combinations. The lead combinations developed using this novel approach mediated marked enhancements in efficacy and safety compared to randomly formulated combinations in multiple breast cancer models (*53*). Moreover, because this process was based on experimental data and not modeling, the optimized drug combinations were implicitly validated.

This review will first examine some of the promising advances that have been made with respect to ND-based applications in biology and medicine. In highlighting the potential of NDs as translationally relevant platforms for drug delivery and imaging, this review will also examine new multidisciplinary opportunities to systematically optimize combinatorial therapy. This will collectively have an impact on both nano and non-nano drug development to ensure that the most effective medicines possible are being translated into the clinic.

UNIQUE SURFACES OF NDs

NDs have several unique properties that make them a promising nanomaterial for biomedical applications. These include unique electrostatic properties, a chemically inert core, and a tunable surface. The ND surface can be modified with a wide variety of functional groups to control interaction with water molecules as well as biologically relevant conjugates. In particular, the unique truncated octahedral shape of DNDs influences facet-specific surface electrostatic potentials (Fig. 1) and the anisotropic distribution of functional groups, such as carboxyl groups. These properties mediate the formation of favorable DND aggregate sizes and drug adsorption capacity (*36*, *38*). Depending on the shape and structure of DNDs, the frequency of (111) and (100) surfaces will vary and along with it the overall surface electrostatic potentials. For a typical truncated octahedral DND used for drug delivery and imaging applications, the (100) and (100)/(111) edges exhibit strong positive potential. The graphitized (111) surfaces exhibit either strong negative potentials or a more neutral potential because of a slight asymmetry of the truncated octahedral DNDs. These unique facet- and shape-dependent electrostatic properties result in favorable DND aggregate sizes through the interaction of negatively charged $(111)^-$ facets with neutral $(111)^0$ or neutral $(110)^0$ facets. In initial preclinical studies, this unique property of ordered ND self-aggregation was shown to contribute substantially to the improved efficacy of drug-resistant tumor therapy (*37*). This served as a vital foundation for the experimental

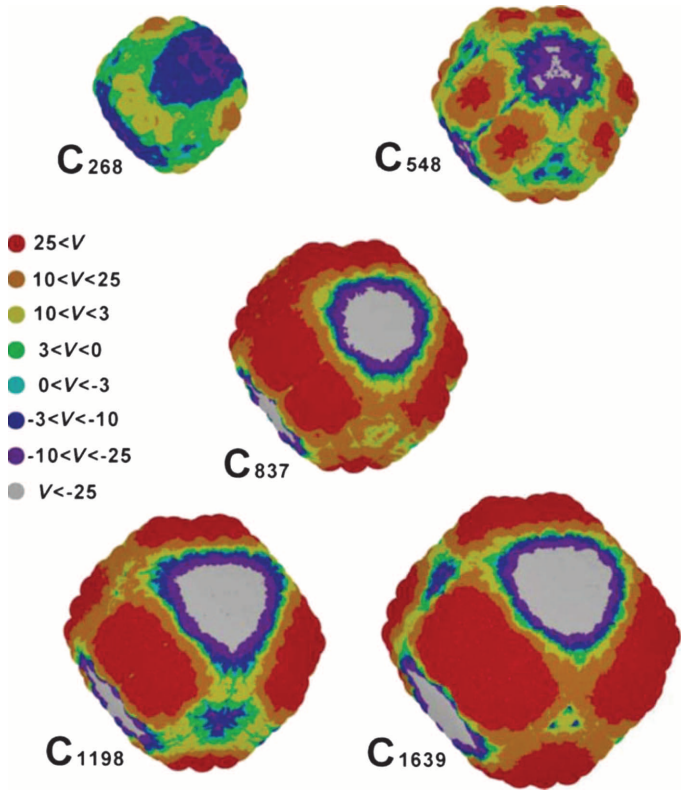

Fig. 1. Unique electrostatic properties of NDs. Analysis of the surface electrostatic potential of truncated octahedral NDs reveals that there is a strong relationship between the shape of the ND facet surfaces and electrostatic potential. (100) surfaces, as well as the (100)/(111) edges, exhibit strong positive potential, whereas graphitized (111) surfaces exhibit strong negative potentials. Reproduced from A. S. Barnard, M. Sternberg, Crystallinity and surface electrostatics of diamond nanocrystals. *J. Mater. Chem.* **17**, 4811 (2007), with permission from The Royal Society of Chemistry.

observation of DND aggregates, particularly the DND-anthracycline complexes for cancer therapy. Of note, the aggregate sizes (~80 nm in diameter) were shown to be critically important for improved tumor therapy. Specifically, the limited clearance effects of the reticuloendothelial system on the DND clusters resulted in a 10-fold increase in circulatory half-life and markedly improved intratumoral drug retention because of this aggregation (*54*, *55*). Therefore, favorable DND aggregate sizes combined with high adsorption capacity allow for efficient drug loading while maintaining a suitable ND-drug complex size for effective passive targeted therapy. This ultimately results in increased efficacy and safety of ND-based cancer therapy approaches (*55*).

ND-BASED IMAGING

NDs, both DND and FND, are also being widely used for imaging applications. Each class of diamond has unique surface or structural features that markedly improve their performance as imaging agents compared to clinical and nanoparticle standards (Fig. 2) (*56*–*59*). In addition to the improvements in magnetic resonance imaging mentioned in the introduction, a recent breakthrough using FNDs pertained to the sustained labeling of lung stem cells (LSCs) to track their engraftment and regenerative potential after lung tissue injury in a murine model (*60*). LSCs are important mediators of epithelial tissue regeneration in vivo as well as regulators of lung tissue homeostasis. Tracking LSCs, however, has been difficult because of the photobleaching and toxicity observed with conventional agents, which can impede the differentiation capabilities or viability of the LSCs. A recent study by Wu *et al.* has demonstrated stable tracking of LSC with fluorescent NDs, confirming LSC localization to the terminal bronchioles after transplantation (Fig. 2B). The NDs were excited by green-yellow light, and the integration of negatively charged nitrogen-vacancy centers resulted in stable far-red emission at a 15-ns lifetime. Because conventional agents have fluorescent lifetimes in the range of 1 to 4 ns, ND fluorescence could be easily differentiated from tissue autofluorescence using fluorescence lifetime imaging microscopy (FLIM). LSCs were screened for the CD54 and CD157 markers to ensure their capacity for differentiation, and further studies confirmed that the cells were from a hematopoietic lineage. Fluorescent NDs incubated with $CD45^{-}CD54^{+}CD157^{+}$ cells were readily endocytosed with no apparent exocytosis. After tail-vein injection of the ND-containing LSCs, their engraftment and differentiation capabilities were unimpaired, resulting in improved localization and epithelial regeneration at the sites of lung injury compared to saline control. This was an important advance because of the sustained LSC monitoring enabled by the photostability and biocompatibility of the fluorescent NDs.

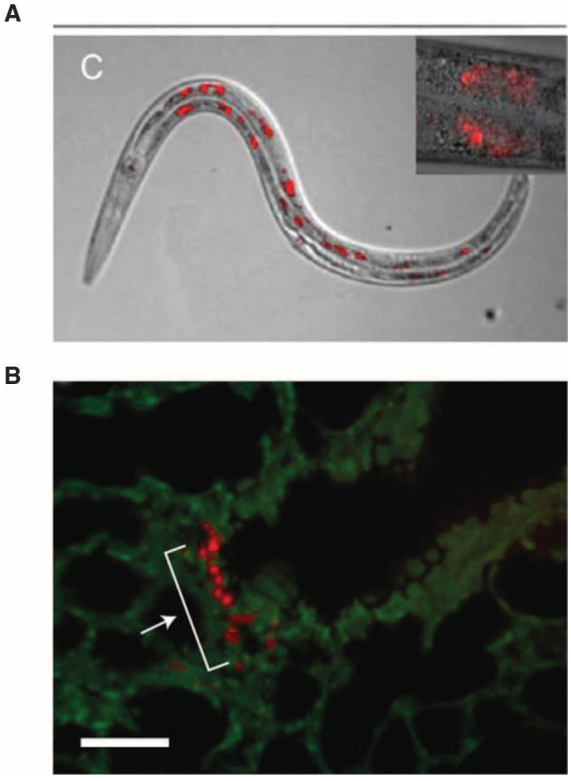

Fig. 2. Imaging applications of FND fluorescent NDs. (**A**) *C. elegans* fed with dextran-coated fluorescent NDs. Reprinted (adapted) with permission from N. Mohan, C.-S. Chen, H.-H. Hsieh, Y.-C. Wu, H.-C. Chang, In vivo imaging and toxicity assessments of fluorescent nanodiamonds in *Caenorhabditis elegans*. *Nano-Lett.* **10**, 3692 (2010/09/08, 2010). Copyright 2010 American Chemical Society. (**B**) Engraftment of fluorescent ND-labeled LSCs in a lung injury mouse model. Adapted with permission from Macmillan Publishers Ltd.: T.-J. Wu *et al.*, Tracking the engraftment and regenerative capabilities of transplanted LSCs using fluorescent NDs. *Nat. Nanotechnol.* **8**, 682 (09//print, 2013), copyright 2013.

ND-BASED DRUG DELIVERY

ND drug delivery has received significant attention because of the facile nature of functionalizing their surfaces with drug compounds, particularly anthracyclines. The anthracycline class of compounds, which include doxorubicin, epirubicin, and daunorubicin, among others, are potent DNA intercalating agents that are used in most chemotherapy regimens. Although anthracyclines have effective anticancer activity, they are also extremely toxic. They induce myelosuppression (which is the dose-limiting side effect of chemotherapy), mediate cardiotoxicity that can result in heart failure, can lead to superinfections, and may markedly increase the risk of developing acute myelogenous leukemia (*61*). Early studies successfully formulated ND-doxorubicin compounds (NDX) through physisorption, enabling potent drug binding and subsequent release without the need to chemically modify the drug itself (*62*, *63*). The NDX compound was subsequently validated in a broad array of cancer models that ranged from in vitro through preclinical in vivo models. Most notably, given that the problem of drug resistance accounts for greater than 90% of tumor treatment failure in metastatic cancer, NDX was tested against two highly drug-resistant cancer models: the 4T1 breast cancer model and the LT2-M liver cancer model (*54*). These tumors are known to express ABC (ATP-binding casette) transporter proteins that mediate drug efflux, markedly reducing the efficacy of chemotherapy with unmodified drugs. This lack of drug retention also results in elevated levels of toxicity. The initial stages of NDX preclinical validation involved the administration of NDs alone to confirm that they were well tolerated in murine models. High ND levels (20 mg) resulted in no apparent increase in serum alanine aminotransferase (ALT) levels, an indicator that the NDs do not cause liver toxicity. In addition, these same dosages did not cause an increase in serum interleukin-6 levels, demonstrating an absence of systemic toxicity as

well. After the initial validation of ND biocompatibility and intracellular retention, verapamil blocking assays were performed, which confirmed that the NDX, compared to unmodified doxorubicin (Dox), was retained longer in 4T1, LT2-M, Huh7, and MDA-MB-231 breast cancer cells. Pharmacokinetic analysis of NDX revealed an observed first phase half-life of 8.43 hours for NDX compared to 0.83 hours for Dox alone. Drug efficacy studies demonstrated a clear decrease in tumor size with NDX administration compared to free Dox administration. In 4T1 tumors, NDX administration (100 μg equivalence) again resulted in markedly reduced tumor sizes compared to the administration of Dox alone. Of note, the administration of Dox alone at 100 μg showed virtually no efficacy, with tumor sizes on the order of those observed with saline control treatment. When the Dox dosage was increased to 200 μg, all of the mice experienced early mortality. When NDX at 200-μg Dox equivalence was administered, all of the mice survived the entire duration of the study, with the tumors being the smallest among all of the test conditions observed. This confirmed that the NDX platform improved therapeutic efficacy against highly drug-resistant tumors and also markedly enhanced drug tolerance, all without the need to chemically modify Dox. Furthermore, the intravenous administration of NDX resulted in no apparent myelosuppression, whereas Dox alone resulted in a substantial decrease in white blood cell count. This finding confirmed the existence of a potent ND-Dox interaction such that premature drug elution did not take place even after systemic injection.

Whereas the NDX compound represented a passive form of Dox delivery, actively targeted ND drug delivery has also been demonstrated. Antibodies against the epidermal growth factor receptor (EGFR) were conjugated to fluorescently labeled NDs with bifunctional cross-linkers for subsequent targeting. Introducing epidermal growth factor (EGF) as a control to block targeting confirmed the improved specificity of delivery in the EGFR-overexpressing MDA-MB-231 breast cancer cell line compared to the MCF7 breast cancer cell line, which does not overexpress EGFR (*64*). Preclinical validation of EGFR targeting was demonstrated with a liposome-encapsulated ND-epirubicin complex. In this iteration of a targeted ND drug delivery complex, the EGFR antibodies were conjugated onto the surface of the liposome, which in turn was used to encapsulate the ND-epirubicin compounds. In mice with MDA-MB-231 tumors, the targeted ND complexes mediated complete tumor regression to the point where they were no longer detectable. The administration of epirubicin alone at 150 μg resulted in early mortality, whereas EGFR-targeted ND delivery of epirubicin at the same dosage resulted in complete animal survival and tumor regression (Fig. 3A) (*46*).

The properties of ND delivery of anthracyclines that allow ND-anthracycline complexes to overcome ABC transporter–mediated drug resistance also lend NDs as a suitable drug delivery platform for effectively treating cancer stem cells (CSCs) (*45*, *65*). Chemoresistance, including ABC transporter–mediated resistance, is often linked to CSCs and is a major mechanism by which these tumor-initiating cells escape traditional therapy and contribute to recurrence (*66*–*68*). This is particularly true for hepatic cancers where chemoresistant and metastatic CSCs have been identified and isolated by expression of these ABC transporter proteins (*69*–*71*). Overexpression of ABC transporter proteins is clinically linked to poorer drug response, including to epirubicin, in hepatic cancers (*72*, *73*). Delivery of epirubicin by NDs was demonstrated to overcome this mechanism of resistance in CSCs and more effectively kill CSCs compared to epirubicin alone (Fig. 3, B and C) (*45*). Treatment with epirubicin alone resulted in a positive selection of hepatic CSCs and in respectively 8.13- and 3.88-fold increases in vitro and in vivo in the frequency of tumor-initiating CSCs among tumor cells that survived drug treatment. In contrast, similar treatment with ND-epirubicin resulted in respectively 3.4- and 5.46-fold decreases in vitro and in vivo in the frequency of tumor-initiating CSCs among remaining tumor cells after ND-drug treatment. This translated into decreased tumor colony formations in vitro as well as a lack of secondary tumor formation in vivo, demonstrating effective elimination of key tumor-initiating CSCs after ND-epirubicin treatment.

Although ND-based drug delivery against cancer remains one of the most developed biomedical applications, tissue engineering and antimicrobial applications are also promising fields in which NDs may also have a therapeutic role (*74*–*85*). Thin-film nanocrystalline diamond (NCD) surfaces were functionalized with growth factors, such as bone morphogenetic protein-2 (BMP-2), through physisorption to promote localized bone formation (*86*). BMP-2–functionalized hydrophilic NCD surfaces were able to promote osteogenic induction in human stromal cells in vitro. In vivo studies with BMP-2–functionalized NCD-coated implants in sheep revealed long-term retention of BMP-2 at the site of implantation compared to control implants. This translated into greater bone formation around the BMP-2–functionalized NCD-coated implant by 4 weeks after implantation. The addition of NDs to copolymer scaffolds can also increase the hydrophilicity of the scaffold to promote the attachment, proliferation, and differentiation of bone marrow stromal cells in vitro and new bone formation in vivo (*87*). Further functionalization with physisorption of BMP-2 to NDs in copolymer scaffolds promoted de novo bone formation in models of mandibular defects in vivo, demonstrating the potential of integrating NDs into tissue-engineering disease applications (*41*).

The versatility of ND surface functionalization and the anisotropic distribution of charges on the ND surface also lend the ND platform to antimicrobial applications. NDs can be functionalized with saccharides to detect and capture bacteria to effectively diagnose and treat infections (*88*). Additionally, NDs can be partially oxidized to mediate potent antimicrobial activity against both Gram-negative and Gram-positive bacteria (*89*). The antimicrobial activity is likely mediated by both the delivery of reactive oxygen species to bacteria cellular components and the alteration of bacterial surfaces by anisotropic distribution of charges of bacteria-interacting NDs. These studies, in addition to those addressing ND drug delivery in cancer, demonstrate that NDs are a promising nanomaterial for a wide array of biomedical applications.

ND BIODISTRIBUTION AND TOXICITY

As NDs progress toward clinical translation, an increasing body of work has explored their biodistribution and biocompatibility properties in vitro and in vivo (*90*, *91*). Dextran- and bovine serum albumin–functionalized FND tracking in the *Caenorhabditis elegans* model has been used to characterize their safety and excretion mechanisms in living organisms (Fig. 2A) (*44*). Observation of ND consumption or microinjection and resulting stress response and reproductive function assessed acute and long-term tolerance in these *C. elegans* preclinical models. The nuclear translocation of the DAF-16 transcription factor served as a stress readout. No apparent toxicity was observed after ND consumption, and gonadal injection resulted in FND presence in worm offspring.

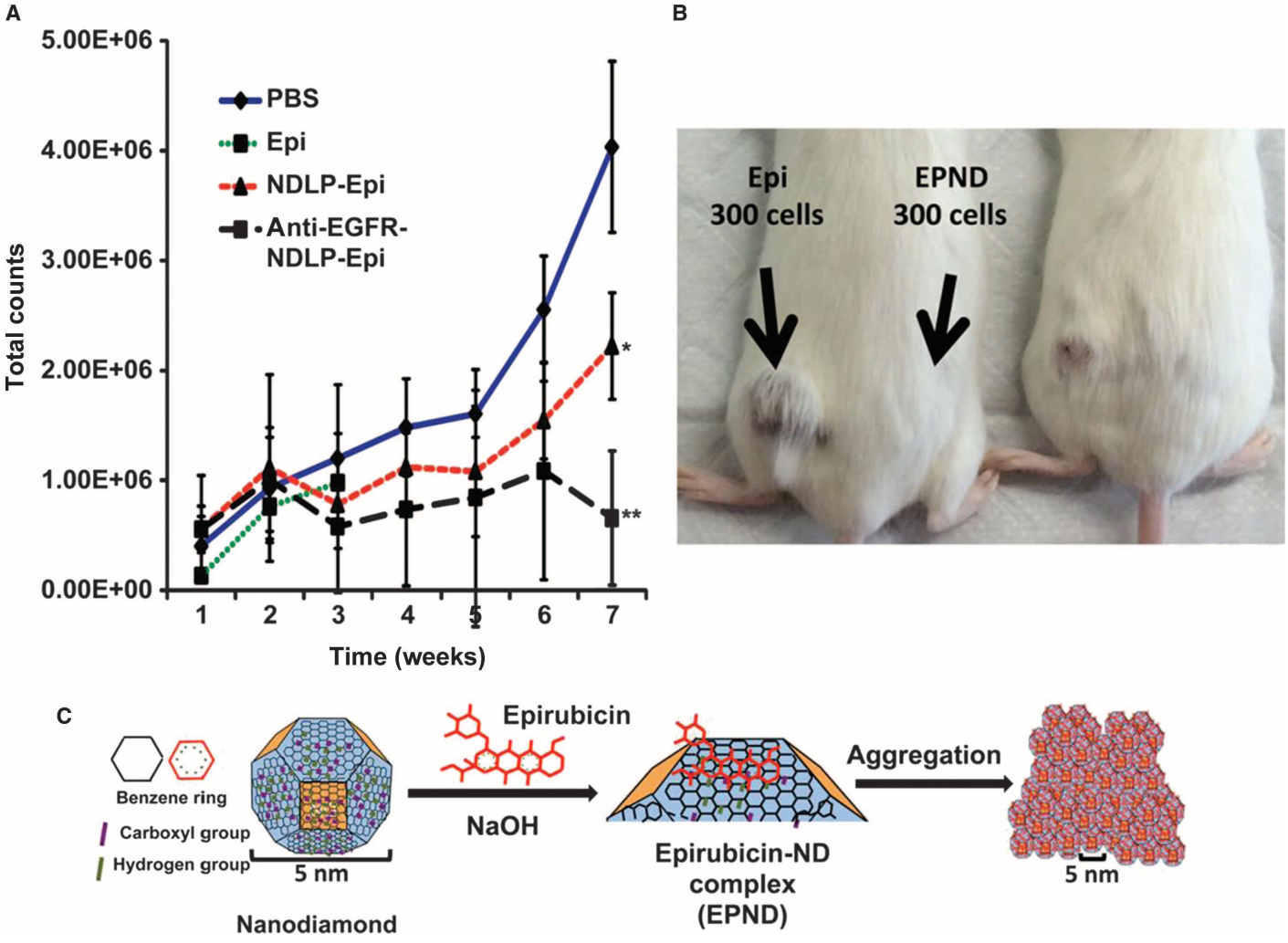

Fig. 3. ND-anthracycline drug delivery in cancer. (**A**) EGFR-targeted delivery of ND-epirubicin (anti-EGFR-NDLP-Epi) against breast cancer cells demonstrated increased efficacy compared to untargeted ND-epirubicin (NDLP-Epi) and unmodified epirubicin (Epi) while retaining the increased safety that results from ND conjugation of epirubicin. Reprinted with permission from WILEY. (**B**) Treatment of hepatic tumor–bearing mice with ND-epirubicin (EPND) efficiently killed hepatic CSCs and prevented secondary tumor formation seen after treatment with unmodified epiruibicin (Epi). (**C**) A schematic model of ND-epirubicin complex formation and aggregation. Reprinted (adapted) with permission from X. Wang *et al.*, Epirubicin-adsorbed nanodiamonds kill chemoresistant hepatic cancer stem cells. *ACS Nano* **8**, 12151 (2014/12/23, 2014). Copyright 2014 American Chemical Society.

Biodistribution studies in mice intravenously injected with fluorescent dye–labeled NDs revealed initial accumulation of NDs in the lung, spleen, liver, and kidneys. Rapid clearance was observed from the lung followed by more gradual clearance of NDs from the spleen, liver, and kidney over a 10-day period. A strong fluorescently labeled ND signal visible from the bladder suggested efficient excretion of NDs (*54*). Biodistribution studies with DNDs radiolabeled with ^{18}F radionuclide and analyzed in mice and rats by positron emission tomography (PET) confirm these results. Radiolabeled NDs were detected primarily in the lung and urine and, to a lesser degree, in the liver and spleen 2 hours after administration (*92*). Biodistribution studies with other carbon-based nanoparticles reveal similarities as well as differences in organ accumulation and excretion of these nanoparticles. Similar to fluorescently labeled NDs, fluorescent carbon dots accumulated mostly in the mouse bladder, kidney, and liver 4 hours after intravenous injection (*21*). Radiolabeled graphene oxide also primarily accumulated in the mouse liver and spleen after intraperitoneal injections but was unable to be excreted from the body, as evidenced by minimal signal in the kidney. Graphene oxide particles were also detected in mouse livers 30 days after intraperitoneal injection (*93*). Whereas CNTs have been observed to be capable of being excreted and even observed by electron microscopy in the urine of treated mice, a comparison study of radiolabeled NDs and CNTs revealed biodistribution differences. CNTs were primarily observed in the lung, whereas NDs were quickly cleared from the lung and found in the liver and spleen (*94*, *95*). Further studies are being conducted to address this observation and to determine the impact of this long-term retention of nanocarbons in the lungs on granuloma formation and chronic pulmonary toxicity (*96*).

Additional studies have sought to examine the cellular mechanisms that are activated after ND exposure to provide deeper insight into the dose-dependent tolerance of NDs at the cellular and preclinical levels. Several of these studies have demonstrated that the NDs are well tolerated even at high dosages. Although prior work has been conducted to monitor potential hematotoxicity, comprehensive in vivo serum toxicity panels in another study resulted in no apparent changes in serum markers (*46*, *97*, *98*). This study and others serve as important indicators that the NDs are well tolerated at multiple dosages in a wide variety of cell lines and a diverse range of animal models.

More recently, a study has been conducted on the cellular compatibility of DNDs, FND NDs, NDs with surface amine groups, and NDs physisorbed with daunorubicin, an anthracycline chemotherapy (*99*). HeLa cervical cancer cells and HepG2 liver cancer cells were selected because of their prevalence as toxicity and drug efficacy testing platforms. After their incubation with the ND subtypes, the cells were examined for indications of cell death, including onset of apoptosis, metabolic states, reduction in drug toxicity from ND sequestering effects, and gene expression profiles.

To assess the biocompatibility of the ND subtypes being investigated, a broad range of assays was conducted. The caspase-3/7 assay was used to measure the potential onset of apoptosis. Cell metabolism was examined using an XTT (2,3-bis[2-methoxy-4-nitro-5-sulfophenyl]-2*H*-tetrazolium-5-carboxanilide inner salt) assay, indications of cellular toxicity were assessed using a lactate dehydrogenase assay, and gene expression profiles were evaluated through quantitative real-time polymerase chain reaction. Key findings from this study showed that high doses (250 μg/ml) of all ND subtypes did not have a negative impact on viability in either cell line. Transcriptional regulation studies demonstrated that incubation of HepG2 cells with NDs at a dose of 25 μg/ml did not result in significant changes in gene expression levels of *Ki-67*, *Bax*, and *c-Myc* genes. This indicates the absence of apoptotic and antiproliferative effects or a cellular stress response. Overall, this represented among the most comprehensive studies of ND safety to date.

Recently, comparative in vitro studies have also been conducted with graphene, CNTs, and NDs to understand the similarities and differences in nanocarbon toxicity (*100*). Whereas CNTs and graphene exhibited similar rates of toxicity with increasing carbon concentration, ND administration appeared to show less toxicity. To further understand the mechanism of nanocarbon toxicity, liposomal leakage studies and toxicogenomic analysis were conducted. The effect of different nanocarbons on liposomal leakage was explored to determine if membrane damage was a possible explanation for any nanocarbon-related toxicity. NDs, CNTs, and graphene could all adsorb onto the surface of liposomes without disrupting the lipid bilayer, suggesting that membrane disruption is not a contributing mechanism to the limited toxicity observed with nanocarbons. Toxicogenomic analysis of nanotitanium dioxide, carbon black, CNTs, and fullerenes in bacteria, yeast, and human cells revealed structure-specific mechanisms of toxicity among nanomaterials, as well as other nanocarbons (*101*). Although both CNTs and fullerenes failed to induce oxidative damage as observed in nanomaterials such as nanotitanium dioxide, they were both capable of inducing DNA double-stranded breaks (DSBs) in eukaryotes. However, the specific mechanisms of DSBs remain unclear because differences in activation of pathway-specific DSB repair genes were found between the two nanocarbons. These studies give an initial understanding of ND and nanocarbon toxicity to continue on a pathway toward clinical implementation and first-in-human use, and comprehensive nonhuman primate studies of ND toxicity are currently under way.

TRANSLATION OF NANOMEDICINE THROUGH COMBINATION THERAPY

For all therapeutics moving from bench to bedside, including NDs and nanomedicine, additional development beyond cellular and animal models of efficacy and toxicity is needed. As these therapeutics are absorbed into drug development pipelines, they will invariably be integrated into combination therapies. This strategy of combinatorial medicine has been recognized by the industry as being essential in various disease areas (for example, pulmonary artery hypertension, cardiovascular disease, diabetes, arthritis, chronic obstructive pulmonary disease, HIV, tuberculosis) and especially oncology (*102*–*110*). How these combinations can be rationally designed so that safety and efficacy are maximized is still a major challenge, and current strategies have only contributed to the increasing cost of new drug development. The inefficiencies in developing and validating suitable combinations lie not only in the empirical clinical testing of these combinations in the clinic but also in the time and resources spent in the clinic. Examples of the way these trials are conducted provide important insight into how optimization of combination therapy can be improved.

For clinical trials conducted and listed on ClinicalTrials.gov from 2008 to 2013, 25.6% of oncology trials contained combinations, compared to only 6.9% of non-oncology trials (*110*). Within each disease area, viral diseases had the next highest percentage of combination trials conducted after oncology at 22.3%, followed by digestive diseases (18.6%), cardiovascular diseases (8.5%), pathological conditions (5.7%), and neurological diseases (5.4%). Because most of the combination trials were performed in oncology, the following clinical examples will display how empirical testing of therapeutic combinations is conducted in this disease area. In many instances, including the following clinical examples, the MTD of the drugs as single agents is often directly used in combinations. This is done without using other methods to determine the best dosing of each drug before use in a particular combination. This empirical approach can lead to poor results due to compounded toxic side effects of the individual therapeutics, unpredictability of other complications, and/or less than optimal efficacies due to the combination of the drugs.

A recent phase 1 study (NCT01400451) looked at the combination of ipilimumab, a monoclonal antibody targeted against CTLA-4, and vemurafanib, a BRAF inhibitor targeting the V600E mutation (*111*). Both therapeutics are approved for single use in melanoma. Because their inhibition pathways are different, the use of both in combination was a natural progression. In this study, both therapeutics were used at the MTD, which resulted in dose-limiting toxicities (DLTs) that unfortunately led to early termination of the study. In another immunotherapy study, a phase 1 study of ipilimumab combined with another V600E BRAF inhibitor, dabrafenib, and mitogen-activated or extracellular signal–regulated protein kinase kinase inhibitor, trametinib, was also terminated early because of grade 4 intestinal perforation in two of the seven patients and grade 3 dose-limiting colitis (*112*). The doublet combination of ipilimumab with the BRAF inhibitor dabrafenib did not show any DLTs, and an expansion cohort was in the process of being enrolled. These first two examples show that direct combination of therapeutics at their MTD without any initial studies looking

at appropriate dosing for the combination may result in toxicity, ultimately preventing the use of the combination. In addition, the second example shows that combinations using molecules that may target the same mutation and pathway may not have the same types of toxic side effects, demonstrating that the differences in combinations using similar classes of therapeutics need to be monitored. In an infectious disease and oncology example using a traditional oncology phase 1 3 + 3 dose escalation design, non–ritonavir-based HAART (highly active antiretroviral therapy) with standard sunitinib therapy (50 mg/day) (treatment arm 1) was compared with the combination of sunitinib in HIV-positive patients receiving ritonavir-based HAART (treatment arm 2) (NCT00890747) (*111*). Patients in treatment arm 1 tolerated treatment without any observed DLT. Treatment arm 2 had DLT at a sunitinib dose of 37.5 mg, with three of five patients having grade 3 neutropenia. This showed that patients on ritonavir could combine the use of sunitinib with ritonavair-based HAART, but that it should be given at a lower dose of sunitinib when used in combination.

These three examples, and many more, demonstrate how clinical trials for combination therapy are often conducted either at the MTD for each therapeutic or with patients being dosed empirically without clear guidelines. Although nanomedicines have yet to be used in many combination therapy trials, they will inevitably join the other types of therapeutic classes in use for combination. Therefore, whereas the current strategy of determining combinatorial drug use has resulted in many combination therapies used to date, it is clearly not the most efficient method and can still be significantly optimized. On the basis of the trend of increasing use of combination therapy in nanomedicine and in broader drug development, as well as the challenges that are faced in determining optimized combination therapies to use, a new paradigm using systematically designed drug combinations needs to be identified. This would be a much needed tool that the pharmaceutical industry is ready to embrace in their efforts to define new combinations that may help their product lifecycle management, or "evergreening," an important part of many companies.

The concept of evergreening is a widely used approach in the pharmaceutical industry to retain patent protection and rent-earning rights on protected compounds with imminent expiry dates (*113*–*115*). This concept includes formulating new drug combinations containing soon-to-be generic compounds to create new patents that may extend the financial lifetime of the drug. Whereas this process may result in intended or unexpected improvements to the safety and/or efficacy of treatment, there is debate about whether these are measures that the drug manufacturers are purposefully taking to prevent generic drug makers from producing these compounds. If so, this may ultimately lead to restricted competition and limitations in the availability of lower-priced medicines to the general population, causing controversy over the concept of suboptimal evergreening.

The application of nanotechnology to novel formulation and delivery has become a highly active area of evergreening strategies. The capacity for nanotechnology to modify properties such as pharmacokinetics, oral bioavailability, drug toxicity and efficacy, and others may result in substantial growth in nanomedicine development. This is particularly true as patent cliffs approach for some of the most profitable medicines in the world. Challenges from both patent-holding and generics companies have been raised in an effort to either promote competition in the pharmaceutical industry, on the one hand, or potentially suppress generic entry on the other. Regardless of the continued controversy surrounding the practice of evergreening, a new challenge that has arisen concerning both sides of the debate involves the need to truly optimize new combinations, both nano and non-nano. This will be necessary to successfully address the issues of maximizing efficacy and safety for the good of public health, as well as meeting the increasing thresholds of patentability. To address this challenge, a key advance at the intersection of nanotechnology and engineering optimization has opened doors to simultaneously optimizing and de-risking the drug development pipeline using phenotype to drive the rational design of combination therapy.

PERSONALIZING AND OPTIMIZING NANOMEDICINE DRUG DEVELOPMENT

Innovative advances in functionalizing nanoparticles combined with multiple classes of therapeutic agents have improved efficacy over monotherapy with nanomedicine. However, the process of globally optimizing combination therapies has thus far been challenging, if not impossible. Dosing levels of the drugs in combination are a major factor in determining the efficacy and toxicity of therapy. Hence, there is a nearly infinite number of possible drug dose combinations that can be designed when conventional screening or predictive approaches are used. Emerging strategies are continually being explored with regard to integrating several therapies with a single class of nanoparticle carriers or the use of several different classes of nanoparticle carriers to mediate combinatorial nanomedicine (*49*, *50*, *52*). These strategies have shown that the delivery of multiple compounds using nanoparticles has resulted in early indications of improved efficacy and toxicity. Therefore, a platform technology that is applicable to all types of nanoparticles and is capable of rationally and systematically optimizing these approaches toward globally optimized safety and efficacy across the in vitro, in vivo, and translational stages of drug development would represent a major advance.

High-throughput screening is a valuable in vitro approach that can use brute force to identify drug combinations that enable the most favorable outcome from those that have been tested. Limitations arise, however, when attempts to simultaneously optimize multiple outcomes, including several safety and efficacy parameters, are made. Aside from a limitless number of combinations that would need to be tested, primary sample testing is likely to be ruled out because of inadequate sample availability. Other efforts to develop optimal drug administration conditions have included the use of pharmacokinetic modeling, median-effect methods to assess drug synergism and antagonism, prediction-based genomic modeling, and mechanism-based systems biology approaches (*116*–*118*). However, the use of these approaches to design drug combinations can result in limitations on the maximum number of drugs that can be used within the combination, mixtures that are rendered ineffective because of resistance, and the inability to optimize on the basis of undruggable mechanistic data. All of these approaches are also subject to significant risks during the development of both nanotechnology-modified and unmodified drugs. The inability to definitively determine optimal drug dose ratios during each stage of testing and development coupled with the confounding aspects of the mechanisms used for drug design commonly result in clinical trial failure.

Recently, Phenotypic Personalized Medicine–Drug Development (PPM-DD) has been developed as a mechanism-independent and modelless platform that uses experimental data to formulate phenotype-based

drug response landscapes (*119*–*122*). As such, mechanistic properties such as signaling pathway behavior, drug-drug interactions, pharmacokinetics, and heterogeneity are innately accounted for using the PPM-DD approach. It is important to note that PPM-DD does not require the use of feedback control, predictive algorithms and modeling, or a pharmacogenetics platform. Instead, it uses experimental data to formulate phenotypic maps to systematically and rapidly identify optimal drug combinations during each stage of the drug development roadmap that ranges from in vitro through in vivo and to translational stages. More specifically, the in vitro stage is used to broadly explore the systematic formulation of novel and optimized initial drug combinations and to narrow down the drugs and lead combinations of initial interest. Subsequent in vivo validation is conducted to reoptimize the drug dose ratios at the preclinical level. Lead combinations can then be further optimized in the translational setting. The ability to properly determine optimal drug dose ratios from discovery and preclinical validation through translation can provide a definitive pathway toward achieving population response rates that will far supersede those that are currently observed with conventionally designed drug combinations.

The first version of PPM-DD was termed Feedback System Control.I (FSC.I). This system used an iterative search process that previously used a search/feedback algorithm to guide experimental validation of combinations to rapidly find a combination that performed optimally both in vitro and in vivo, even from prohibitively large pools of possible combinations (*119*, *123*). The term Feedback System Control is a remnant of the first version of the platform, and subsequent iterations were no longer based on feedback. Therefore, the recent development of PPM-DD [previously referred to as Feedback System Control.II (FSC.II)] resulted in an experimentally driven optimization platform that inherently accounts for all mechanistic components of disease (for example, cellular signaling networks, patient heterogeneity, genomic aberrations) to formulate drug combinations that culminate in an optimal phenotypic output (*53*, *124*).

With regard to optimizing nanomedicine drug combinations, PPM-DD was first applied to ND-based combination therapy to produce four-drug combinations composed of NDX, ND-mitoxantrone, ND-bleomycin, and unmodified paclitaxel to maximize the therapeutic window of breast cancer therapy (Fig. 4). In this study, ND-drug combinations were administered to three breast cancer cell lines (MDA-MB-231, BT20, and MCF-7) and three control cell lines (H9C2 cardiomyocytes, MCF10A breast fibroblasts, and IMR-90 lung fibroblasts). PPM-DD was capable of creating phenotypic maps based on a limited number of therapeutic window assays to immediately identify the combination that simultaneously resulted in optimal cancer cell apoptosis and control cell viability. Because these mechanism-free maps are based on phenotypic experimental data, the optimized combinations were innately validated. Key findings from this study showed that phenotypically optimized ND-drug combinations outperformed single ND-drug and unmodified drug administration, optimized unmodified drug combinations, and randomly selected ND-drug combinations. This study showed that PPM-DD uses a parallel experimentation-optimization process that requires only a small number of test subjects, making preclinical optimization possible. In addition, PPM-DD uniquely identified the global optimum drug dose ratio for efficacy and safety in this study, a key achievement that would not have been possible using conventional dose escalation and additive design. Therefore, PPM-DD effectively provides a pathway toward implicitly de-risked drug development for population-optimized response rates.

Another recent study has demonstrated the capacity to use phenotypic data to pinpoint optimal drug combinations that maximize therapeutic efficacy while minimizing adverse effects. The phenotype-based experiments were performed for hepatic cancers and normal hepatocytes, and they revealed novel combinations of glucose metabolism inhibitors through phenotypic-based experiments without the need for previous mechanistic information (Fig. 5) (*124*). Increased glucose uptake and reprogramming of cellular energy metabolism, the Warburg effect, are hallmarks of many cancers, including hepatic cancers, and linked to tumor progression and poorer outcome (*125*–*127*). The key mechanisms that are required for enhanced glucose metabolism–mediated tumor progression are often complex and thus difficult to target therapeutically by traditional drug development methods (*128*). After a multiparameter high-content screen to identify glucose metabolism inhibitors that also specifically inhibit hepatic cancer cell proliferation but have minimal effects on normal hepatocytes, PPM-DD was implemented to identify optimal therapeutic combinations. Using a minimal number of experimental combinations, this study was able to identify both synergistic and antagonistic drug interactions in two-drug and three-drug combinations that effectively killed hepatic cancer cells through inhibition of glucose metabolism. Optimal drug combinations involved phenotypically identified synergistic drugs that inhibit distinct signaling pathways, such as the Janus kinase 3 (JAK3) and cyclic adenosine monophosphate–dependent protein kinase (PKA)/ cyclic guanosine monophosphate–dependent protein kinase (PKG) pathways, which were not previously known to be involved in hepatic cancer glucose metabolism. As such, this platform not only optimized drug combinations in a mechanism-independent manner but also identified previously unreported druggable molecular mechanisms that synergistically contribute to tumor progression.

The core concept of PPM-DD represents a major paradigm shift for the optimization of nanomedicine or unmodified drug combination optimization because of its mechanism-independent foundation. Therefore, genotypic and other potentially confounding mechanisms are considered a function of the resulting phenotype, which serves as the endpoint readout used for optimization. To further illustrate the foundation of this powerful platform, the phenotype of a biological complex system can be classified as resulting tumor size, viral loads, cell viability, apoptotic state, a therapeutic window representing a difference between viable healthy cells and viable cancer cells, a desired range of serum markers that indicate that a drug is well tolerated, or a broad range of other physical traits. In fact, phenotype can be classified as the simultaneous observation of several phenotypic traits at the same time to result in a multiobjective endpoint. For the purpose of optimizing drug combinations in drug development, we have discovered that efficacy can be represented by the following expression and can be optimized independent of knowledge associated with the mechanisms that drive disease onset and progression (*53*):

$$V(\mathbf{s},\mathbf{x}) = V(\mathbf{s},0) + \sum_k a_k x_k + \sum_l b_l x_l^2 + \sum_m \sum_n c_{mn} x_m x_n + \text{high order elements}$$

The elements of this expression represent disease mechanisms that can be prohibitively complex and as such are unknown, particularly when mutation, heterogeneity, and other elements are considered, including completely differentiated behavior between individuals and subpopulations even when genetic variations are shared. Therefore, the

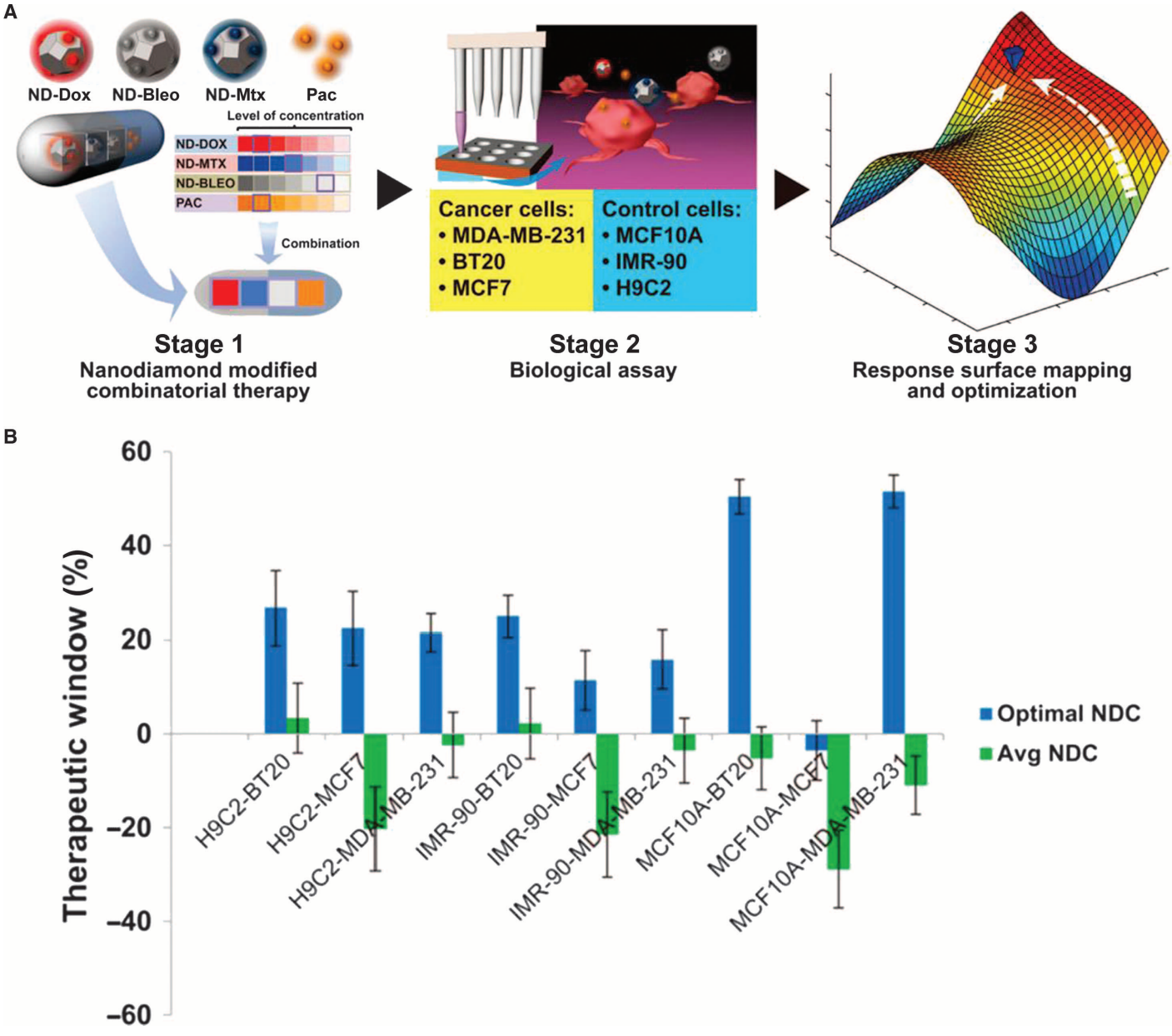

Fig. 4. PPM-DD–optimized ND-drug combinations. (**A**) A schematic model of the PPM experimental framework. Dox, doxorubicin; Bleo, bleomycin; Mtx, mitoxantrone; Pac, paclitaxel. (**B**) PPM-derived optimal ND-drug combinations (NDC) outperform a random sampling of NDCs in effective therapeutic windows of treatment of cancer cells compared to control cells. Reprinted (adapted) with permission from H. Wang *et al.*, Mechanism-independent optimization of combinatorial nanodiamond and unmodified drug delivery using a phenotypically driven platform technology. *ACS Nano* (2015/02/17, 2015). Copyright 2014 American Chemical Society.

overall treatment outcome can be represented by the difference in efficacy before and after treatment. It is important to note that the resulting quadratic algebraic sequence is a function of the doses only and is hence mechanism-free. Unprecedented capabilities in optimizing combinatorial drug development can then be achieved through facile sampling of various dose combinations to rapidly identify the algebraic series coefficients, resulting in the most potent drug dose combination according to phenotype only. Figures 4C and 5D harness this quadratic algebraic equation to provide a global analysis of the drug-drug interaction map in a wide dose range. This map visually demonstrates that dose dependence in drug design can have a profound impact on drug synergism and antagonism. A systematic combination therapy development platform such as the PPM-DD approach can rationally pinpoint the specific drug dose ratios that result in globally optimal treatment outcomes, not just the best outcome for a specific sample set. The number or types of drugs within the combination do not limit this approach. Therefore, PPM-DD can develop combinations containing multiple nanoformulated therapies and unmodified therapies and is not confined to conventional triplet or doublet therapy formulation (*53*, *55*, *119*, *120*, *123*, *124*, *129*–*131*).

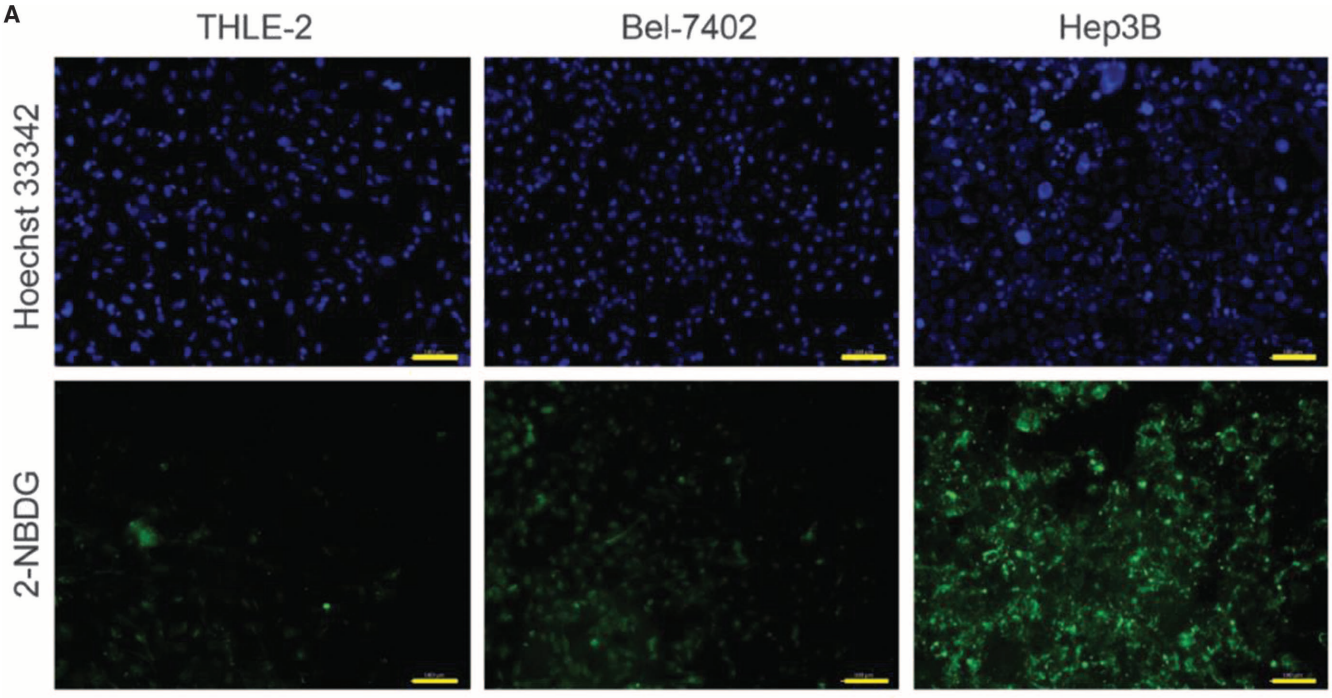

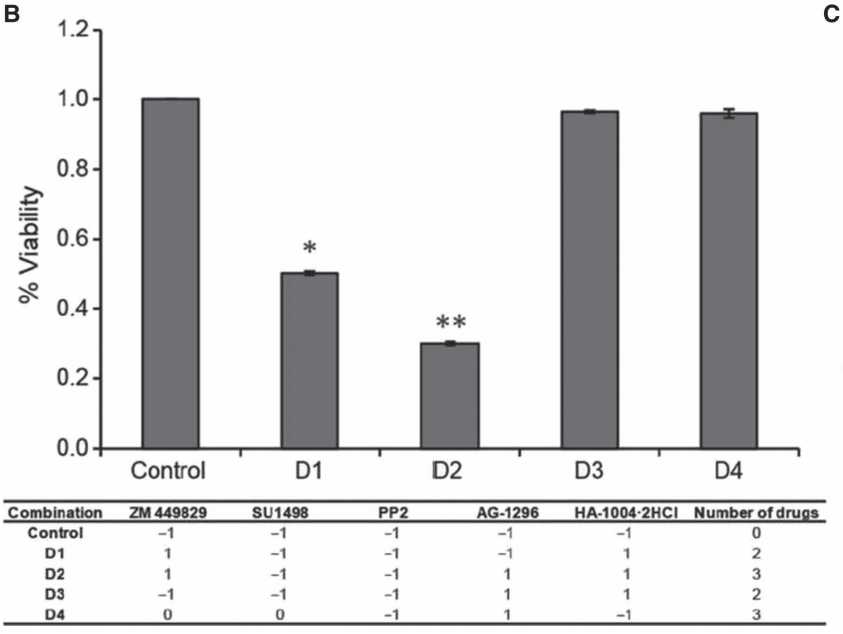

Combination	ZM 449829	SU1498	PP2	AG-1296	HA-1004·2HCl	Number of drugs
Control	−1	−1	−1	−1	−1	0
D1	1	−1	−1	−1	1	2
D2	1	−1	−1	1	1	3
D3	−1	−1	−1	1	1	2
D4	0	0	−1	1	−1	3

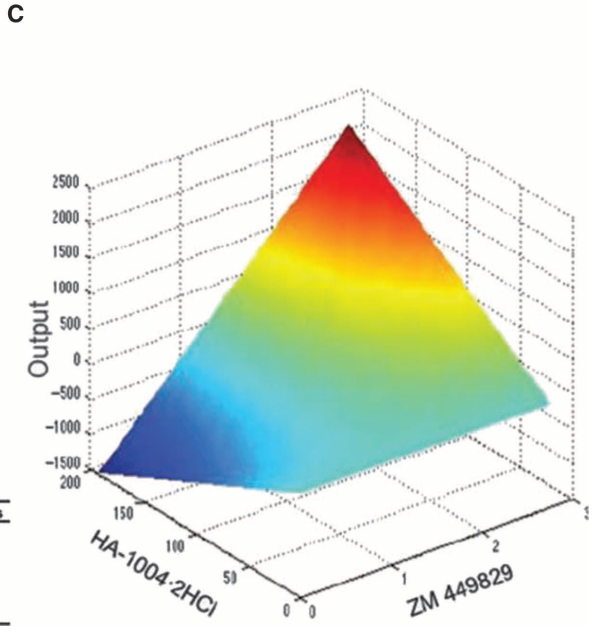

Fig. 5. PPM-DD–optimized drug combinations against hepatic cancers. (**A**) Hepatic cancer cells, such as Hep3B, exhibit enhanced uptake of glucose and glucose analogs (2-NBDG) compared to normal hepatocytes (THLE-2) and other hepatic cancer cells (Bel-7402). (**B**) Inhibition of hepatic cancer cell proliferation by PPM-DD–optimized two-drug (D1) and three-drug (D2) combinations were compared to PPM-DD–derived nonsignificant combinations (D3 and D4) in vitro. (**C**) Response surface plots of predicted outputs after ZM 449829 and HA-1004·2HCl reveal a synergistic relationship between the two drugs. Figures reprinted with permission from SAGE Publications.

The PPM-DD platform can effectively achieve multiobjective and optimal outcomes without the need for mechanistic information. However, given the ability to identify these optimal phenotypic outcomes, this platform can be paired with other discovery platforms to then pinpoint the specific mechanisms responsible for these phenotypes. This makes PPM-DD an extremely powerful platform that can transform the drug development process.

CONCLUDING REMARKS

On the basis of important studies that comprehensively characterized the uniquely faceted electrostatic surface properties of DNDs, as well as the nitrogen-vacancy center properties of FNDs, rapid progress has been made in the areas of ND-based imaging and therapy. In the area

of cancer therapy, passive and actively targeted ND-anthracycline complexes have proven to be scalable platforms for hard-to-treat cancers that increase the efficacy and safety of chemotherapy. ND-based imaging agents enabling preclinical tracking of LSC engraftment and markedly increasing per-gadolinium relaxivity provide a strong foundation for continued development for both basic and translational applications. As more delivery platforms within the nanomedicine field are clinically validated, their role in transforming the pharmaceutical industry will become more defined. Monotherapy mediated by nanomedicine vehicles has already resulted in improved efficacy and safety over clinical standards in recent human trials. Combination therapy is another area where nanotechnology is poised to have an impact on patient care in an important way. However, this also raises challenges of how these combinations can be rationally designed, given the enormous limitations associated with identifying proper drug dose parameters from an infinite parameter space.

To circumvent the limitations of conventional combinatorial design approaches, a paradigm-shifting platform that uses phenotype to systematically identify globally optimized drug combinations was utilized to formulate ND-based and unmodified drug combinations. These rationally developed therapies substantially outperformed randomly sampled drug combinations with respect to efficacy and safety. Furthermore, the use of experimental data to formulate phenotypic response maps innately validated the lead combinations. Combining nanomaterials with specific drug compounds using engineering optimization platforms can truly optimize drug dose combinations for defined indications. This will lead to unprecedented advances in patient treatment outcomes against the most serious diseases of our time.

OUTLINE OF UNRESOLVED QUESTIONS

The field of nanomedicine has given rise to a collection of promising nanomaterial platforms. As nanomedicine-modified monotherapies continue to move into the clinic following important initial findings from first-in-human studies, the next frontier will involve the clinical implementation of combination nanotherapies. The inefficiency of dose escalation– or additive design–based formulation of combination therapies is a challenge that has persistently confronted the broader pharmaceutical industry. It is evident that the nanomedicine field will need to address this barrier, particularly as nanotechnology drug delivery and imaging agents increase in complexity. Nanomedicines are now being designed to simultaneously carry several classes of payloads, or different classes of nanomaterials are being co-delivered as a combination. This review used the ND platform to illustrate specific examples, such as magnetic resonance imaging and cancer therapy, where NDs immensely outperform conventional modalities. A recent advance at the multidisciplinary interface of engineering systems identification and ND drug delivery resulted in the demonstration that ND-drug combinations could be effectively optimized for multiple parameters in a mechanism-independent fashion. This work simultaneously addressed the challenges of optimal drug discovery and the use of nanomedicine to even further boost efficacy and safety. This review addressed the following pervasive challenges and breakthroughs in drug development:

- Nano-based monotherapy implementation in the clinic has made important advances in improving treatment outcomes. Nanotechnology-based modification of drugs is also becoming increasingly prevalent as the pharmaceutical industry looks for ways to innovate existing drugs. Combination therapy represents the next stage of nanomedicine implementation.
- As the costs of drug development continue to climb, a strategy to pinpoint which nanomaterial platforms are best suited for specific drug and imaging compounds and indications must be developed.
- NDs have emerged as promising materials for imaging and therapy. Their specific clinical role will depend on continued toxicity and efficacy studies, but initial studies in magnetic resonance imaging and anthracycline delivery are promising.
- Combination therapy is currently designed using additive formulation. This makes it virtually impossible to optimize therapy, which has a negative impact on public health. When simultaneously addressing the prohibitively large number of possible drug combinations using current methods and requiring that the efficacy and safety are both optimal, the parameter space is simply too large.
- The emergence of PPM-DD, previously referred to as the FSC.II technology, has now made it possible to design globally optimal drug combinations, even with multiobjective criteria, using nanotherapeutics and non-nano therapeutics. PPM-DD is capable of optimizing combination therapy design at each stage of development. This implicitly de-risks the drug development process because the globally optimal drug dose ratios are identified from an empirically constructed phenotypic map.
- The demonstration of PPM-DD-based optimization in ND combination therapy optimization resulted in globally maximal cancer cell death and minimal healthy cell death. This was all accomplished in a mechanism-independent fashion using a small sample of phenotypic assays. This signified a major advance for nano-enhanced combination therapy.

REFERENCES AND NOTES

1. X. Xu, K. Xie, X. Q. Zhang, E. M. Pridgen, G. Y. Park, D. S. Cui, J. Shi, J. Wu, P. W. Kantoff, S. J. Lippard, R. Langer, G. C. Walker, O. C. Farokhzad, Enhancing tumor cell response to chemotherapy through nanoparticle-mediated codelivery of siRNA and cisplatin prodrug. *Proc. Natl. Acad. Sci. U.S.A.* **110**, 18638–18643 (2013).
2. N. A. Peppas, J. Z. Hilt, A. Khademhosseini, R. Langer, Hydrogels in biology and medicine: From molecular principles to bionanotechnology. *Adv. Mater.* **18**, 1345–1360 (2006).
3. J. Hrkach, D. Von Hoff, M. M. Ali, E. Andrianova, J. Auer, T. Campbell, D. De Witt, M. Figa, M. Figueiredo, A. Horhota, S. Low, K. McDonnell, E. Peeke, B. Retnarajan, A. Sabnis, E. Schnipper, J. J. Song, Y. H. Song, J. Summa, D. Tompsett, G. Troiano, T. Van Geen Hoven, J. Wright, P. LoRusso, P. W. Kantoff, N. H. Bander, C. Sweeney, O. C. Farokhzad, R. Langer, S. Zale, Preclinical development and clinical translation of a PSMA-targeted docetaxel nanoparticle with a differentiated pharmacological profile. *Sci. Transl. Med.* **4**, 128ra139 (2012).
4. T. Dvir, M. Bauer, A. Schroeder, J. H. Tsui, D. G. Anderson, R. Langer, R. Liao, D. S. Kohane, Nanoparticles targeting the infarcted heart. *Nano Lett.* **11**, 4411–4414 (2011).
5. X. Zhang, M. D. Do, K. Dean, P. Hoobin, I. M. Burgar, Wheat-gluten-based natural polymer nanoparticle composites. *Biomacromolecules* **8**, 345–353 (2007).
6. M. M. Abdel-Mottaleb, D. Neumann, A. Lamprecht, Lipid nanocapsules for dermal application: A comparative study of lipid-based versus polymer-based nanocarriers. *Eur. J. Pharm. Biopharm.* **79**, 36–42 (2011).
7. S. A. Jensen, E. S. Day, C. H. Ko, L. A. Hurley, J. P. Luciano, F. M. Kouri, T. J. Merkel, A. J. Luthi, P. C. Patel, J. I. Cutler, W. L. Daniel, A. W. Scott, M. W. Rotz, T. J. Meade, D. A. Giljohann, C. A. Mirkin, A. H. Stegh, Spherical nucleic acid nanoparticle conjugates as an RNAi-based therapy for glioblastoma. *Sci. Transl. Med.* **5**, 209ra152 (2013).
8. X.-Q. Zhang, X. Xu, R. Lam, D. Giljohann, D. Ho, C. A. Mirkin, Strategy for increasing drug solubility and efficacy through covalent attachment to polyvalent DNA–nanoparticle conjugates. *ACS Nano.* **5**, 6962–6970 (2011).
9. A. Bianco, K. Kostarelos, M. Prato, Applications of carbon nanotubes in drug delivery. *Curr. Opin. Chem. Biol.* **9**, 674–679 (2005).
10. Z. Liu, K. Chen, C. Davis, S. Sherlock, Q. Cao, X. Chen, H. Dai, Drug delivery with carbon nanotubes for in vivo cancer treatment. *Cancer Res.* **68**, 6652–6660 (2008).

11. A. K. Patri, I. J. Majoros, J. R. Baker Jr., Dendritic polymer macromolecular carriers for drug delivery. *Curr. Opin. Chem. Biol.* **6**, 466–471 (2002).
12. A. M. Gobin, M. H. Lee, N. J. Halas, W. D. James, R. A. Drezek, J. L. West, Near-infrared resonant nanoshells for combined optical imaging and photothermal cancer therapy. *Nano Lett.* **7**, 1929–1934 (2007).
13. M. E. Davis, J. E. Zuckerman, C. H. J. Choi, D. Seligson, A. Tolcher, C. A. Alabi, Y. Yen, J. D. Heidel, A. Ribas, Evidence of RNAi in humans from systemically administered siRNA via targeted nanoparticles. *Nature* **464**, 1067–1070 (2010).
14. C. Wang, J. Li, C. Amatore, Y. Chen, H. Jiang, X. M. Wang, Gold nanoclusters and graphene nanocomposites for drug delivery and imaging of cancer cells. *Angew. Chem. Int. Ed. Engl.* **50**, 11644–11648 (2011).
15. R. P. Feazell, N. Nakayama-Ratchford, H. Dai, S. J. Lippard, Soluble single-walled carbon nanotubes as longboat delivery systems for platinum(IV) anticancer drug design. *J. Am. Chem. Soc.* **129**, 8438–8439 (2007).
16. N. W. Kam, M. O'Connell, J. A. Wisdom, H. Dai, Carbon nanotubes as multifunctional biological transporters and near-infrared agents for selective cancer cell destruction. *Proc. Natl. Acad. Sci. U.S.A.* **102**, 11600–11605 (2005).
17. L. Wang, Q. Sun, X. Wang, T. Wen, J. J. Yin, P. Wang, R. Bai, X. Q. Zhang, L. H. Zhang, A. H. Lu, C. Chen, Using hollow carbon nanospheres as a light-induced free radical generator to overcome chemotherapy resistance. *J. Am. Chem. Soc.* **137**, 1947–1955 (2015).
18. P. Chaudhuri, A. Paraskar, S. Soni, R. A. Mashelkar, S. Sengupta, Fullerenol–cytotoxic conjugates for cancer chemotherapy. *ACS Nano.* **3**, 2505–2514 (2009).
19. W. Li, Z. Zhang, B. Kong, S. Feng, J. Wang, L. Wang, J. Yang, F. Zhang, P. Wu, D. Zhao, Simple and green synthesis of nitrogen-doped photoluminescent carbonaceous nanospheres for bioimaging. *Angew. Chem. Int. Ed. Engl.* **52**, 8151–8155 (2013).
20. Q. Liu, B. Guo, Z. Rao, B. Zhang, J. R. Gong, Strong two-photon-induced fluorescence from photostable, biocompatible nitrogen-doped graphene quantum dots for cellular and deep-tissue imaging. *Nano Lett.* **13**, 2436–2441 (2013).
21. S. T. Yang, L. Cao, P. G. Luo, F. Lu, X. Wang, H. Wang, M. J. Meziani, Y. Liu, G. Qi, Y. P. Sun, Carbon dots for optical imaging in vivo. *J. Am. Chem. Soc.* **131**, 11308–11309 (2009).
22. A. S. Barnard, Self-assemblyin nanodiamond agglutinates. *J. Mater. Chem.* **18**, 4038–4041 (2008).
23. A. S. Barnard, Diamond standard in diagnostics: Nanodiamond biolabels make their mark. *Analyst* **134**, 1751–1764 (2009).
24. A. Adnan, R. Lam, H. Chen, J. Lee, D. J. Schaffer, A. S. Barnard, G. C. Schatz, D. Ho, W. K. Liu, Atomistic simulation and measurement of pH dependent cancer therapeutic interactions with nanodiamond carrier. *Mol. Pharm.* **8**, 368–374 (2010).
25. Y. Y. Hui, L.-J. Su, O. Y. Chen, Y.-T. Chen, T.-M. Liu, H.-C. Chang, Wide-field imaging and flow cytometric analysis of cancer cells in blood by fluorescent nanodiamond labeling and time gating. *Sci. Rep.* **4**, 5574 (2014).
26. Y. Y. Hui, C.-L. Cheng, H.-C. Chang, Nanodiamonds for optical bioimaging. *J. Phys. D Appl. Phys.* **43**, 374021 (2010).
27. L. P. McGuinness, Y. Yan, A. Stacey, D. A. Simpson, L. T. Hall, D. Maclaurin, S. Prawer, P. Mulvaney, J. Wrachtrup, F. Caruso, R. E. Scholten, L. C. Hollenberg, Quantum measurement and orientation tracking of fluorescent nanodiamonds inside living cells. *Nat. Nanotechnol.* **6**, 358–363 (2011).
28. J. Tisler, G. Balasubramanian, B. Naydenov, R. Kolesov, B. Grotz, R. Reuter, J.-P. Boudou, P. A. Curmi, M. Sennour, A. Thorel, M. Börsch, K. Aulenbacher, R. Erdmann, P. R. Hemmer, F. Jelezko, J. Wrachtrup, Fluorescence and spin properties of defects in single digit nanodiamonds. *ACS Nano* **3**, 1959–1965 (2009).
29. O. Faklaris, V. Joshi, T. Irinopoulou, P. Tauc, M. Sennour, H. Girard, C. Gesset, J.-C. Arnault, A. Thorel, J.-P. Boudou, P. A. Curmi, F. Treussart, Photoluminescent diamond nanoparticles for cell labeling: Study of the uptake mechanism in mammalian cells. *ACS Nano* **3**, 3955–3962 (2009).
30. A. Alhaddad, C. Durieu, G. Dantelle, E. Le Cam, C. Malvy, F. Treussart, J.-R. Bertrand, Influence of the internalization pathway on the efficacy of siRNA delivery by cationic fluorescent nanodiamonds in the Ewing sarcoma cell model. *PLOS One* **7**, e52207 (2012).
31. Y. Liang, M. Ozawa, A. Krueger, A general procedure to functionalize agglomerating nanoparticles demonstrated on nanodiamond. *ACS Nano* **3**, 2288–2296 (2009).
32. S. Heyer, W. Janssen, S. Turner, Y.-G. Lu, W. S. Yeap, J. Verbeeck, K. Haenen, A. Krueger, Toward deep blue nano hope diamonds: Heavily boron-doped diamond nanoparticles. *ACS Nano* **8**, 5757–5764 (2014).
33. V. N. Mochalin, O. Shenderova, D. Ho, Y. Gogotsi, The properties and applications of nanodiamonds. *Nat. Nanotechnol.* **7**, 11–23 (2012).
34. H. A. Girard, T. Petit, S. Perruchas, T. Gacoin, C. Gesset, J. C. Arnault, P. Bergonzo, Surface properties of hydrogenated nanodiamonds: A chemical investigation. *Phys. Chem. Chem. Phys.* **13**, 11517–11523 (2011).
35. W. Dexters, E. Bourgeois, M. Nesladek, J. D'Haen, E. Goovaerts, K. Haenen, Molecular orientation of lead phthalocyanine on (100) oriented single crystal diamond surfaces. *Phys. Chem. Chem. Phys.* **17**, 9619–9623 (2015).
36. A. S. Barnard, M. Sternberg, Crystallinity and surface electrostatics of diamond nanocrystals. *J. Mater. Chem.* **17**, 4811–4819 (2007).
37. L.-Y. Chang, E. Osawa, A. S. Barnard, Confirmation of the electrostatic self-assembly of nanodiamonds. *Nanoscale* **3**, 958–962 (2011).
38. L. Lai, A. S. Barnard, Anisotropic adsorption and distribution of immobilized carboxyl on nanodiamond. *Nanoscale* **6**, 14185–14189 (2014).
39. A. S. Barnard, M. C. Per, Size and shape dependent deprotonation potential and proton affinity of nanodiamond. *Nanotechnology* **25**, 445702 (2014).
40. L. M. Manus, D. J. Mastarone, E. A. Waters, X.-Q. Zhang, E. A. Schultz-Sikma, K. W. MacRenaris, D. Ho, T. J. Meade, GD(III)-nanodiamond conjugates for MRI contrast enhancement. *Nano Lett.* **10**, 484–489 (2010).
41. S. Suliman, Z. Xing, X. Wu, Y. Xue, T. O. Pedersen, Y. Sun, A. P. Døskeland, J. Nickel, T. Waag, H. Lygre, A. Finne-Wistrand, D. Steinmüller-Nethl, A. Krueger, K. Mustafa, Release and bioactivity of bone morphogenetic protein-2 are affected by scaffold binding techniques in vitro and in vivo. *J. Control. Release* **197**, 148–157 (2015).
42. H.-J. Kim, K. Zhang, L. Moore, D. Ho, Diamond nanogel-embedded contact lenses mediate lysozyme-dependent therapeutic release. *ACS Nano* **8**, 2998–3005 (2014).
43. G. Balasubramanian, I. Y. Chan, R. Kolesov, M. Al-Hmoud, J. Tisler, C. Shin, C. Kim, A. Wojcik, P. R. Hemmer, A. Krueger, T. Hanke, A. Leitenstorfer, R. Bratschitsch, F. Jelezko, J. Wrachtrup, Nanoscale imaging magnetometry with diamond spins under ambient conditions. *Nature* **455**, 648–651 (2008).
44. N. Mohan, C.-S. Chen, H.-H. Hsieh, Y.-C. Wu, H.-C. Chang, In vivo imaging and toxicity assessments of fluorescent nanodiamonds in *Caenorhabditis elegans*. *Nano Lett.* **10**, 3692–3699 (2010).
45. X. Wang, X. C. Low, W. Hou, L. N. Abdullah, T. B. Toh, M. Mohd Abdul Rashid, D. Ho, E. K.-H. Chow, Epirubicin-adsorbed nanodiamonds kill chemoresistant hepatic cancer stem cells. *ACS Nano* **8**, 12151–12166 (2014).
46. L. Moore, E. K.-H. Chow, E. Osawa, J. M. Bishop, D. Ho, Diamond-lipid hybrids enhance chemotherapeutic tolerance and mediate tumor regression. *Adv. Mater.* **25**, 3532–3541 (2013).
47. H. Meng, W. X. Mai, H. Zhang, M. Xue, T. Xia, S. Lin, X. Wang, Y. Zhao, Z. Ji, J. I. Zink, A. E. Nel, Codelivery of an optimal drug/siRNA combination using mesoporous silica nanoparticles to overcome drug resistance in breast cancer in vitro and in vivo. *ACS Nano* **7**, 994–1005 (2013).
48. H. Meng, M. Xue, T. Xia, Z. Ji, D. Y. Tarn, J. I. Zink, A. E. Nel, Use of size and a copolymer design feature to improve the biodistribution and the enhanced permeability and retention effect of doxorubicin-loaded mesoporous silica nanoparticles in a murine xenograft tumor model. *ACS Nano* **5**, 4131–4144 (2011).
49. Z. J. Deng, S. W. Morton, E. Ben-Akiva, E. C. Dreaden, K. E. Shopsowitz, P. T. Hammond, Layer-by-layer nanoparticles for systemic codelivery of an anticancer drug and siRNA for potential triple-negative breast cancer treatment. *ACS Nano* **7**, 9571–9584 (2013).
50. T. Jiang, R. Mo, A. Bellotti, J. Zhou, Z. Gu, Gel–liposome-mediated co-delivery of anticancer membrane-associated proteins and small-molecule drugs for enhanced therapeutic efficacy. *Adv. Funct. Mater.* **24**, 2295–2304 (2014).
51. R. Mo, T. Jiang, R. DiSanto, W. Tai, Z. Gu, ATP-triggered anticancer drug delivery. *Nat. Commun.* **5**, 3364 (2014).
52. G. von Maltzahn, J.-H. Park, K. Y. Lin, N. Singh, C. Schwöppe, R. Mesters, W. E. Berdel, E. Ruoslahti, M. J. Sailor, S. N. Bhatia, Nanoparticles that communicate in vivo to amplify tumour targeting. *Nat. Mater.* **10**, 545–552 (2011).
53. H. Wang, D.-K. Lee, K.-Y. Chen, J.-Y. Chen, K. Zhang, A. Silva, C.-M. Ho, D. Ho, Mechanism-independent optimization of combinatorial nanodiamond and unmodified drug delivery using a phenotypically driven platform technology. *ACS Nano* **9**, 3332–3344 (2015).
54. E. K. Chow, X.-Q. Zhang, M. Chen, R. Lam, E. Robinson, H. Huang, D. Schaffer, E. Osawa, A. Goga, D. Ho, Nanodiamond therapeutic delivery agents mediate enhanced chemoresistant tumor treatment. *Sci. Transl. Med.* **3**, 73ra21 (2011).
55. E. K. Chow, D. Ho, Cancer nanomedicine: From drug delivery to imaging. *Sci. Transl. Med.* **5**, 216rv4 (2013).
56. T. A. Dolenko, S. A. Burikov, A. M. Vervald, I. I. Vlasov, S. A. Dolenko, K. A. Laptinskiy, J. M. Rosenholm, O. A. Shenderova, Optical imaging of fluorescent carbon biomarkers using artificial neural networks. *J. Biomed. Opt.* **19**, 117007 (2014).
57. V. Vaijayanthimala, D. K. Lee, S. V. Kim, A. Yen, N. Tsai, D. Ho, H. C. Chang, O. Shenderova, Nanodiamond-mediated drug delivery and imaging: Challenges and opportunities. *Expert Opin. Drug. Deliv.* **12**, 735–749 (2015).
58. D. A. Simpson, A. J. Thompson, M. Kowarsky, N. F. Zeeshan, M. S. Barson, L. T. Hall, Y. Yan, S. Kaufmann, B. C. Johnson, T. Ohshima, F. Caruso, R. E. Scholten, R. B. Saint, M. J. Murray, L. C. Hollenberg, In vivo imaging and tracking of individual nanodiamonds in drosophila melanogaster embryos. *Biomed. Opt. Express* **5**, 1250–1261 (2014).
59. T. Chen, F. Lu, A. M. Streets, P. Fei, J. Quan, Y. Huang, Optical imaging of non-fluorescent nanodiamonds in live cells using transient absorption microscopy. *Nanoscale* **5**, 4701–4705 (2013).
60. T.-J. Wu, Y.-K. Tzeng, W.-W. Chang, C.-A. Cheng, Y. Kuo, C.-H. Chien, H.-C. Chang, J. Yu, Tracking the engraftment and regenerative capabilities of transplanted lung stem cells using fluorescent nanodiamonds. *Nat. Nanotechnol.* **8**, 682–689 (2013).
61. R. J. Cersosimo, W. K. Hong, Epirubicin: A review of the pharmacology, clinical activity, and adverse effects of an adriamycin analogue. *J. Clin. Oncol.* **4**, 425–439 (1986).

62. H. Huang, E. Pierstorff, E. Osawa, D. Ho, Active nanodiamond hydrogels for chemotherapeutic delivery. *Nano Lett.* **7**, 3305–3314 (2007).
63. R. Lam, M. Chen, E. Pierstorff, H. Huang, E. Osawa, D. Ho, Nanodiamond-embedded microfilm devices for localized chemotherapeutic elution. *ACS Nano* **2**, 2095–2102 (2008).
64. X.-Q. Zhang, R. Lam, X. Xu, E. K. Chow, H.-J. Kim, D. Ho, Multimodal nanodiamond drug delivery carriers for selective targeting, imaging, and enhanced chemotherapeutic efficacy. *Adv. Mater.* **23**, 4770–4775 (2011).
65. T. B. Toh, D. K. Lee, W. Hou, L. N. Abdullah, J. Nguyen, D. Ho, E. K. Chow, Nanodiamond-mitoxantrone complexes enhance drug retention in chemoresistant breast cancer cells. *Mol. Pharm.* **11**, 2683–2691 (2014).
66. T. Kondo, T. Setoguchi, T. Taga, Persistence of a small subpopulation of cancer stem-like cells in the C6 glioma cell line. *Proc. Natl. Acad. Sci. U.S.A.* **101**, 781–786 (2004).
67. P. P. Szotek, R. Pieretti-Vanmarcke, P. T. Masiakos, D. M. Dinulescu, D. Connolly, R. Foster, D. Dombkowski, F. Preffer, D. T. Maclaughlin, P. K. Donahoe, Ovarian cancer side population defines cells with stem cell-like characteristics and Mullerian Inhibiting Substance responsiveness. *Proc. Natl. Acad. Sci. U.S.A.* **103**, 11154–11159 (2006).
68. E. K. Chow, Implication of cancer stem cells in cancer drug development and drug delivery. *J. Lab. Autom.* **18**, 6–11 (2013).
69. T. Chiba, K. Kita, Y. W. Zheng, O. Yokosuka, H. Saisho, A. Iwama, H. Nakauchi, H. Taniguchi, Side population purified from hepatocellular carcinoma cells harbors cancer stem cell–like properties. *Hepatology* **44**, 240–251 (2006).
70. G. M. Shi, Y. Xu, J. Fan, J. Zhou, X. R. Yang, S. J. Qiu, Y. Liao, W. Z. Wu, Y. Ji, A. W. Ke, Z. B. Ding, Y. Z. He, B. Wu, G. H. Yang, W. Z. Qin, W. Zhang, J. Zhu, Z. H. Min, Z. Q. Wu, Identification of side population cells in human hepatocellular carcinoma cell lines with stepwise metastatic potentials. *J. Cancer Res. Clin. Oncol.* **134**, 1155–1163 (2008).
71. E. K. Chow, L. L. Fan, X. Chen, J. M. Bishop, Oncogene-specific formation of chemoresistant murine hepatic cancer stem cells. *Hepatology* **56**, 1331–1341 (2012).
72. Z. Sun, Z. Zhao, G. Li, S. Dong, Z. Huang, L. Ye, H. Liang, J. Qu, X. Ai, W. Zhang, X. Chen, Relevance of two genes in the multidrug resistance of hepatocellular carcinoma: In vivo and clinical studies. *Tumori* **96**, 90–96 (2010).
73. I. O. Ng, C. L. Liu, S. T. Fan, M. Ng, Expression of P-glycoprotein in hepatocellular carcinoma. A determinant of chemotherapy response. *Am. J. Clin. Pathol.* **113**, 355–363 (2000).
74. Z. Zhang, B. Niu, J. Chen, X. He, X. Bao, J. Zhu, H. Yu, Y. Li, The use of lipid-coated nanodiamond to improve bioavailability and efficacy of sorafenib in resisting metastasis of gastric cancer. *Biomaterials* **35**, 4565–4572 (2014).
75. G. Xi, E. Robinson, B. Mania-Farnell, E. F. Vanin, K. W. Shim, T. Takao, E. V. Allender, C. S. Mayanil, M. B. Soares, D. Ho, T. Tomita, Convection-enhanced delivery of nanodiamond drug delivery platforms for intracranial tumor treatment. *Nanomedicine* **10**, 381–391 (2014).
76. J. Xiao, X. Duan, Q. Yin, Z. Zhang, H. Yu, Y. Li, Nanodiamonds-mediated doxorubicin nuclear delivery to inhibit lung metastasis of breast cancer. *Biomaterials* **34**, 9648–9656 (2013).
77. A. D. Salaam, P. Hwang, R. McIntosh, H. N. Green, H. W. Jun, D. Dean, Nanodiamond-DGEA peptide conjugates for enhanced delivery of doxorubicin to prostate cancer. *Beilstein J. Nanotechnol.* **5**, 937–945 (2014).
78. J. Slegerova, M. Hajek, I. Rehor, F. Sedlak, J. Stursa, M. Hruby, P. Cigler, Designing the nanobiointerface of fluorescent nanodiamonds: Highly selective targeting of glioma cancer cells. *Nanoscale* **7**, 415–420 (2015).
79. I. Rehor, K. L. Lee, K. Chen, M. Hajek, J. Havlik, J. Lokajova, M. Masat, J. Slegerova, S. Shukla, H. Heidari, S. Bals, N. F. Steinmetz, P. Cigler, Plasmonic nanodiamonds: Targeted core–shell type nanoparticles for cancer cell thermoablation. *Adv. Healthc. Mater.* **4**, 460–468 (2015).
80. T. Zhang, H. Cui, C. Y. Fang, K. Cheng, X. Yang, H. C. Chang, M. L. Forrest, Targeted nanodiamonds as phenotype-specific photoacoustic contrast agents for breast cancer. *Nanomedicine* **10**, 573–587 (2015).
81. Q. Zhang, V. N. Mochalin, I. Neitzel, I. Y. Knoke, J. Han, C. A. Klug, J. G. Zhou, P. I. Lelkes, Y. Gogotsi, Fluorescent PLLA-nanodiamond composites for bone tissue engineering. *Biomaterials* **32**, 87–94 (2011).
82. Q. Zhang, V. N. Mochalin, I. Neitzel, K. Hazeli, J. Niu, A. Kontsos, J. G. Zhou, P. I. Lelkes, Y. Gogotsi, Mechanical properties and biomineralization of multifunctional nanodiamond-PLLA composites for bone tissue engineering. *Biomaterials* **33**, 5067–5075 (2012).
83. A. Alhaddad, M. P. Adam, J. Botsoa, G. Dantelle, S. Perruchas, T. Gacoin, C. Mansuy, S. Lavielle, C. Malvy, F. Treussart, J. R. Bertrand, Nanodiamond as a vector for siRNA delivery to Ewing sarcoma cells. *Small* **7**, 3087–3095 (2011).
84. L. Grausova, L. Bacakova, A. Kromka, S. Potocky, M. Vanecek, M. Nesladek, V. Lisa, Nanodiamond as promising material for bone tissue engineering. *J. Nanosci. Nanotechnol.* **9**, 3524–3534 (2009).
85. M. Khanal, F. Larsonneur, V. Raks, A. Barras, J. S. Baumann, F. A. Martin, R. Boukherroub, J. M. Ghigo, C. Ortiz Mellet, V. Zaitsev, J. M. Garcia Fernandez, C. Beloin, A. Siriwardena, S. Szunerits, Inhibition of type 1 fimbriae-mediated Escherichia coli adhesion and biofilm formation by trimeric cluster thiomannosides conjugated to diamond nanoparticles. *Nanoscale* **7**, 2325–2335 (2015).
86. F. R. Kloss, R. Gassner, J. Preiner, A. Ebner, K. Larsson, O. Hachl, T. Tuli, M. Rasse, D. Moser, K. Laimer, E. A. Nickel, G. Laschober, R. Brunauer, G. Klima, P. Hinterdorfer, D. Steinmuller-Nethl, G. Lepperdinger, The role of oxygen termination of nanocrystalline diamond on immobilisation of BMP-2 and subsequent bone formation. *Biomaterials* **29**, 2433–2442 (2008).
87. Z. Xing, T. O. Pedersen, X. Wu, Y. Xue, Y. Sun, A. Finne-Wistrand, F. R. Kloss, T. Waag, A. Krueger, D. Steinmuller-Nethl, K. Mustafa, Biological effects of functionalizing copolymer scaffolds with nanodiamond particles. *Tissue Eng. Part A* **19**, 1783–1791 (2013).
88. M. Hartmann, P. Betz, Y. Sun, S. N. Gorb, T. K. Lindhorst, A. Krueger, Saccharide-modified nanodiamond conjugates for the efficient detection and removal of pathogenic bacteria. *Chemistry* **18**, 6485–6492 (2012).
89. J. Wehling, R. Dringen, R. N. Zare, M. Maas, K. Rezwan, Bactericidal activity of partially oxidized nanodiamonds. *ACS Nano* **8**, 6475–6483 (2014).
90. V. Paget, J. A. Sergent, R. Grall, S. Altmeyer-Morel, H. A. Girard, T. Petit, C. Gesset, M. Mermoux, P. Bergonzo, J. C. Arnault, S. Chevillard, Carboxylated nanodiamonds are neither cytotoxic nor genotoxic on liver, kidney, intestine and lung human cell lines. *Nanotoxicology* **8**, 46–56 (2014).
91. Y. A. Huang, C. W. Kao, K. K. Liu, H. S. Huang, M. H. Chiang, C. R. Soo, H. C. Chang, T. W. Chiu, J. I. Chao, E. Hwang, The effect of fluorescent nanodiamonds on neuronal survival and morphogenesis. *Sci. Rep.* **4**, 6919 (2014).
92. S. Rojas, J. D. Gispert, R. Martin, S. Abad, C. Menchon, D. Pareto, V. M. Victor, M. Alvaro, H. Garcia, J. R. Herance, Biodistribution of amino-functionalized diamond nanoparticles. In vivo studies based on ^{18}F radionuclide emission. *ACS Nano* **5**, 5552–5559 (2011).
93. K. Yang, H. Gong, X. Shi, J. Wan, Y. Zhang, Z. Liu, In vivo biodistribution and toxicology of functionalized nano-graphene oxide in mice after oral and intraperitoneal administration. *Biomaterials* **34**, 2787–2795 (2013).
94. Q. Wei, L. Zhan, B. Juanjuan, W. Jing, W. Jianjun, S. Taoli, G. Yi'an, W. Wangsuo, Biodistribution of co-exposure to multi-walled carbon nanotubes and nanodiamonds in mice. *Nanoscale Res. Lett.* **7**, 473 (2012).
95. R. Singh, D. Pantarotto, L. Lacerda, G. Pastorin, C. Klumpp, M. Prato, A. Bianco, K. Kostarelos, Tissue biodistribution and blood clearance rates of intravenously administered carbon nanotube radiotracers. *Proc. Natl. Acad. Sci. U.S.A.* **103**, 3357–3362 (2006).
96. C. A. Poland, R. Duffin, I. Kinloch, A. Maynard, W. A. Wallace, A. Seaton, V. Stone, S. Brown, W. Macnee, K. Donaldson, Carbon nanotubes introduced into the abdominal cavity of mice show asbestos-like pathogenicity in a pilot study. *Nat. Nanotechnol.* **3**, 423–428 (2008).
97. S. Kumari, M. K. Singh, S. K. Singh, J. J. A. Grácio, D. Dash, Nanodiamonds activate blood platelets and induce thromboembolism. *Nanomedicine* **9**, 427–440 (2013).
98. Y. Xing, W. Xiong, L. Zhu, E. Osawa, S. Hussin, L. Dai, DNA damage in embryonic stem cells caused by nanodiamonds. *ACS Nano* **5**, 2376–2384 (2011).
99. L. Moore, V. Grobarova, H. Shen, H. B. Man, J. Micova, M. Ledvina, J. Stursa, M. Nesladek, A. Fiserova, D. Ho, Comprehensive interrogation of the cellular response to fluorescent, detonation and functionalized nanodiamonds. *Nanoscale* **6**, 11712–11721 (2014).
100. X. Y. Zhang, W. B. Hu, J. Li, L. Tao, Y. Wei, A comparative study of cellular uptake and cytotoxicity of multi-walled carbon nanotubes, graphene oxide, and nanodiamond. *Tox. Res.* **1**, 62–68 (2012).
101. J. Lan, N. Gou, C. Gao, M. He, A. Z. Gu, Comparative and mechanistic genotoxicity assessment of nanomaterials via a quantitative toxicogenomics approach across multiple species. *Environ. Sci. Technol.* **48**, 12937–12945 (2014).
102. M. S. Buckley, R. L. Staib, L. M. Wicks, Combination therapy in the management of pulmonary arterial hypertension. *Int. J. Clin. Pract. Suppl.* **179**, 13–23 (2013).
103. R. Smith, T. McCready, S. Yusuf, Combination therapy to prevent cardiovascular disease: Slow progress. *JAMA* **309**, 1595–1596 (2013).
104. G. Derosa, S. Sibilla, Optimizing combination treatment in the management of type 2 diabetes. *Vasc. Health Risk Manag.* **3**, 665–671 (2007).
105. J. Dale, N. Alcorn, H. Capell, R. Madhok, Combination therapy for rheumatoid arthritis: Methotrexate and sulfasalazine together or with other DMARDs. *Nat. Clin. Pract. Rheumatol.* **3**, 450–458 (2007).
106. D. P. Tashkin, G. T. Ferguson, Combination bronchodilator therapy in the management of chronic obstructive pulmonary disease. *Respir. Res.* **14**, 49 (2013).
107. C. P. Passaes, A. Saez-Cirion, HIV cure research: Advances and prospects. *Virology* **454-455**, 340–352 (2014).
108. D. Mitchison, G. Davies, The chemotherapy of tuberculosis: Past, present and future. *Int. J. Tuberc. Lung Dis.* **16**, 724–732 (2012).
109. M. L. Maitland, C. Hudoba, K. L. Snider, M. J. Ratain, Analysis of the yield of phase II combination therapy trials in medical oncology. *Clin. Cancer Res.* **16**, 5296–5302 (2010).
110. M. Wu, M. Sirota, A. J. Butte, B. Chen, Characteristics of drug combination therapy in oncology by analyzing clinical trial data on ClinicalTrials.gov. *Pac. Symp. Biocomput.* **20**, 68–79 (2015).
111. A. Ackerman, O. Klein, D. F. McDermott, W. Wang, N. Ibrahim, D. P. Lawrence, A. Gunturi, K. T. Flaherty, F. S. Hodi, R. Kefford, A. M. Menzies, M. B. Atkins, G. V. Long, R. J. Sullivan, Outcomes of patients with metastatic melanoma treated with immunotherapy prior to or after BRAF inhibitors. *Cancer* **120**, 1695–1701 (2014).

112. J. D. Wolchok, paper presented at the AACR Annual Meeting, Philadelphia, PA, 18 to 22 April 2015.
113. R. Collier, Drug patents: The evergreening problem. *CMAJ* **185**, E385–E386 (2013).
114. C. S. Hemphill, B. N. Sampat, Evergreening, patent challenges, and effective market life in pharmaceuticals. *J. Health Econ.* **31**, 327–339 (2012).
115. R. G. Frank, The ongoing regulation of generic drugs. *N Engl. J Med.* **357**, 1993–1996 (2007).
116. T.-C. Chou, Drug combination studies and their synergy quantification using the Chou-Talalay method. *Cancer Res.* **70**, 440–446 (2010).
117. T.-C. Chou, P. Talalay, Quantitative analysis of dose-effect relationships: The combined effects of multiple drugs or enzyme inhibitors. *Adv. Enzyme Regul.* **22**, 27–55 (1984).
118. L. Hood, J. R. Heath, M. E. Phelps, B. Lin, Systems biology and new technologies enable predictive and preventative medicine. *Science* **306**, 640–643 (2004).
119. P. K. Wong, F. Yu, A. Shahangian, G. Cheng, R. Sun, C.-M. Ho, Closed-loop control of cellular functions using combinatory drugs guided by a stochastic search algorithm. *Proc. Natl. Acad. Sci. U.S.A.* **105**, 5105–5110 (2008).
120. H. Tsutsui, B. Valamehr, A. Hindoyan, R. Qiao, X. Ding, S. Guo, O. N. Witte, X. Liu, C.-M. Ho, H. Wu, An optimized small molecule inhibitor cocktail supports long-term maintenance of human embryonic stem cells. *Nat. Commun.* **2**, 167 (2011).
121. I. Al-Shyoukh, F. Yu, J. Feng, K. Yan, S. Dubinett, C.-M. Ho, J. S. Shamma, R. Sun, Systematic quantitative characterization of cellular responses induced by multiple signals. *BMC Syst. Biol.* **5**, 88 (2011).
122. H. Yu, W. L. Zhang, X. Ding, K. Y. Zheng, C.-M. Ho, K. W. Tsim, Y.-K. Lee, Optimizing combinations of flavonoids deriving from astragali radix in activating the regulatory element of erythropoietin by a feedback system control scheme. *Evid. Based Complement. Alternat. Med.* **2013**, 541436 (2013).
123. A. Weiss, X. Ding, J. van Beijnum, I. Wong, T. Wong, R. Berndsen, O. Dormond, M. Dallinga, L. Shen, R. Schlingemann, R. Pili, C.-M. Ho, P. Dyson, H. van den Bergh, A. Griffioen, P. Nowak-Sliwinska, Rapid optimization of drug combinations for the optimal angiostatic treatment of cancer. *Angiogenesis* **18**, 233–244 (2015).
124. M. B. Mohd Abdul Rashid, T. B. Toh, A. Silva, L. Nurrul Abdullah, C.-M. Ho, D. Ho, E. K.-H. Chow, Identification and optimization of combinatorial glucose metabolism inhibitors in hepatocellular carcinomas. *J. Lab. Autom.* **20**, 423–437 (2015).
125. T. Amann, U. Maegdefrau, A. Hartmann, A. Agaimy, J. Marienhagen, T. S. Weiss, O. Stoeltzing, C. Warnecke, J. Scholmerich, P. J. Oefner, M. Kreutz, A. K. Bosserhoff, C. Hellerbrand, GLUT1 expression is increased in hepatocellular carcinoma and promotes tumorigenesis. *Am. J. Pathol.* **174**, 1544–1552 (2009).
126. O. Warburg, On the origin of cancer cells. *Science* **123**, 309–314 (1956).
127. M. Younes, R. W. Brown, M. Stephenson, M. Gondo, P. T. Cagle, Overexpression of glut1 and glut3 in stage I nonsmall cell lung carcinoma is associated with poor survival. *Cancer* **80**, 1046–1051 (1997).
128. M. O. Yuneva, T. W. Fan, T. D. Allen, R. M. Higashi, D. V. Ferraris, T. Tsukamoto, J. M. Mates, F. J. Alonso, C. Wang, Y. Seo, X. Chen, J. M. Bishop, The metabolic profile of tumors depends on both the responsible genetic lesion and tissue type. *Cell Metab.* **15**, 157–170 (2012).
129. X. Ding, D. J. Sanchez, A. Shahangian, I. Al-Shyoukh, G. Cheng, C.-M. Ho, Cascade search for HSV-1 combinatorial drugs with high antiviral efficacy and low toxicity. *Int. J. Nanomed.* **7**, 2281 (2012).
130. X. Ding, H. Xu, C. Hopper, J. Yang, C. M. Ho, Use of fractional factorial designs in antiviral drug studies. *Qual. Reliab. Eng. Int.* **29**, 299–304 (2013).
131. Y. Honda, X. Ding, F. Mussano, A. Wiberg, C.-M. Ho, I. Nishimura, Guiding the osteogenic fate of mouse and human mesenchymal stem cells through feedback system control. *Sci. Rep.* **3**, 3420 (2013).

Acknowledgments: We acknowledge all of the studies that were not discussed in this review because of space limitations. **Funding:** D.H. gratefully acknowledges support from the National Science Foundation CAREER Award (CMMI-1350197); Center for Scalable and Integrated NanoManufacturing (DMI-0327077); National Science Foundation Awards CMMI-0856492, DMR-1343991, and IIA-1444100; V Foundation for Cancer Research Scholars Award; Wallace H. Coulter Foundation Translational Research Award; National Cancer Institute grant U54CA151880 (the content is solely the responsibility of the authors and does not necessarily represent the official views of the National Cancer Institute or the NIH); Society for Laboratory Automation and Screening Endowed Fellowship; Beckman Coulter Life Sciences; and American Academy of Implant Dentistry Research Foundation under grant number 20150460. E.K.-H.C. gratefully acknowledges support from the National Research Foundation Cancer Science Institute of Singapore RCE Main Grant, National Medical Research Council (NMRC CBRGNIG NMRC/BNIG/2012/2013), and Ministry of Education Academic Research Fund (MOE AcRF Tier 1 T1-2012 Oct-11 and Seed Fund Grant T1-BSRG 2014-05). This work is funded by the NCIS Yong Siew Yoon Research Grant through donations from the Yong Loo Lin Trust. **Author contributions:** D.H., C-H.K.W., and E.K.-H.C. wrote the paper. **Competing Interests:** D.H. and E.K.-H.C. are inventors of pending patents pertaining to ND drug delivery and imaging, as well as the PPM and Feedback System Control (FSC) platforms.

Submitted 7 April 2015
Accepted 20 July 2015
Published 21 August 2015
10.1126/sciadv.1500439

Citation: D. Ho, C.-H. K. Wang, E. K.-H. Chow, Nanodiamonds: The intersection of nanotechnology, drug development, and personalized medicine. *Sci. Adv.* **1**, e1500439 (2015).

ScienceAdvances

Nanodiamonds: The intersection of nanotechnology, drug development, and personalized medicine

Dean HoChung-Huei Katherine WangEdward Kai-Hua Chow

Sci. Adv., 1 (7), e1500439. • DOI: 10.1126/sciadv.1500439

Science Advances (ISSN 2375-2548) is published by the American Association for the Advancement of Science. 1200 New York Avenue NW, Washington, DC 20005. The title *Science Advances* is a registered trademark of AAAS.